Microfluidics for high-throughput quantitative studies of early development

Thomas J. Levario[a], Bomyi Lim[b], Stanislav Y. Shvartsman[b,†], and Hang Lu[a,†]

Affiliations:

[a]School of Chemical & Biomolecular Engineering, Georgia Institute of Technology, Atlanta, GA, USA 30332.

[b]Department of Chemical and Biological Engineering and Lewis-Sigler Institute for Integrative Genomics, Princeton University, Princeton, New Jersey, USA 08544.

Emails:

T.J.L. tlevario3@gatech.edu

B.L. bomyilim@gmail.com

S.Y.S. stas@princeton.edu

H.L. hang.lu@gatech.edu

Microfluidics for quantitative biology

† Correspondence should be directed to H.L. (email:hang.lu@gatech.edu; phone: 404-894-8473) and S.Y.S. (email: stas@princeton.edu; phone: 609-258-4694)

Contents

1. INTRODUCTION

2. FLUORESCENCE MICROSCOPY FOR IMAGING DEVELOPMENT

2.1. Confocal microscopy

2.2. Light-sheet microscopy

3. MICROFLUIDICS AND AUTOMATION FOR MANIPULATING MODELS OF DEVELOPMENT

3.1. *Drosophila*

3.2. *Zebrafish*

3.3. *C. elegans*

3.4. Microfluidics for studying other models of developmental biology

4. IMAGE ANALYSIS SOFTWARE AND COMPUTER VISION FOR DEVELOPMENTAL BIOLOGY

4.1. Automated cell lineaging

4.2. Virtual embryos

4.3. Computer vision for automated phenotyping

5. QUANTITATIVE ANALYSES AND MODELING- A CASE STUDY ON PATTERN FORMATION

6. CONCLUSION

Keywords

Quantitative biology, fluorescence microscopy, automation, computer vision, developmental biology, modeling

Abstract

Developmental biology has traditionally relied on qualitative analyses; recently however, as in other fields of biology, researchers have become increasingly interested in acquiring quantitative knowledge about embryogenesis. Advances in fluorescence microscopy are enabling high-content imaging in live specimen. At the same time, microfluidics and automation technologies are increasing experimental throughput for studying multicellular models of development. Furthermore, computer vision methods for processing and analyzing bioimage data is now leading the way toward quantitative biology. Here, we review advancements in the areas of fluorescence microscopy, microfluidics, and data analysis that are instrumental to performing high-content, high-throughput studies in biology and specifically in development. We will provide a case study discussion on how these techniques have allowed quantitative analysis and modeling of pattern formation in the *Drosophila* embryo.

1. INTRODUCTION

Understanding how biological systems operate macroscopically (e.g. morphogenesis and behavior), and how this is governed by microscopic activities (e.g. gene expression and cell signaling) is a key goal throughout biology. There are many tools available that can be used to address these questions including direct observation of biological processes in living organisms, and to extract meaningful information from what is observed. So-called *in vivo* imaging uses fluorescence microscopy, and in recent years, significant advances in optical sectioning techniques have enabled imaging with high spatiotemporal resolution deep within intact tissues for high-content imaging. In parallel, engineers have been progressing microfluidics technology to enable high-throughput experimentation, and perform tasks that were simply not possible without microfluidic technology. Both high-throughput experimentation and high-content imaging can produce vast amounts of biological imaging data requiring the development of automated image processing and data extraction techniques. In this review, we want to highlight recent advances in the areas of: 1) fluorescence microscopy, 2) microfluidic and automation technology, and 3) image analysis software and computer vision as it pertains to developmental biology. This will be followed by a detailed discussion of a specific application wherein microfluidics-enabled high-throughput imaging enabled quantitative analysis of pattern formation in the developing *Drosophila melanogaster* (from here after referred to as *Drosophila*) embryo. At the end of this review, we hope to convince readers that integrated approaches that combine these techniques will open the door to quantitative developmental biology.

2. FLUORSCENCE MICROSCOPY FOR IMAGING DEVELOPMENT

Fluorescence microscopy, and specifically epifluorescence microscopy, has been the workhorse for imaging-based experiments in biology for hundreds of years. Currently epifluorescence imaging is commonly used, and suitable for addressing many questions in research areas such as behavior, neuroscience, and development. However, epifluorescence microscopy is often insufficient to spatially resolve features deep within the tissues of larger model organisms such as zebrafish and *Drosophila* embryos, or highly diffractive tissues such as cell aggregates. To improve spatial resolution, biologists turn to optical sectioning techniques such as confocal microscopy (1-4) and light-sheet microscopy (5-9).

2.1. Confocal microscopy

Confocal microscopy has been around for several decades, and there are many commercially available systems that make this technique one of the most commonly used method of optical sectioning. Confocal microscopy achieves optical sectioning through the use of a pinhole aperture that acts as a spatial filter to remove out-of-focus light and allowing only the in-focus light to pass through to the detector, which is typically a photomultiplier tube. In point scanning confocal microscopy a light source illuminates the whole specimen, and the final image is constructed by scanning the laser across the focal plane to build up the image pixel by pixel (**Figure 1**). Single-photon confocal microscopy is a powerful tool for acquiring high-resolution images deep within intact tissue, but still has limited imaging depth in highly diffractive tissues such as *Drosophila* embryos. Non-linear optics (NLO), i.e. two-photon excitation, can alleviate some of the scattering issues associated with single-photon excitation, and enable deeper imaging within thick tissues (10). Many studies have utilized two-photon microscopy, and for brevity sake only a few

will be highlighted here. McMahon et al. (11) used two-photon confocal microscopy in order to image ventral furrow formation, collapse, and subsequent mesoderm spreading in live *Drosophila* embryos. Two-photon excitation was used to image these processes at the anterior-posterior center of the embryo from laterally oriented embryos and track cell movements. In a similar application, Wang et al. (12) used two-photon excitation to monitor epithelial invagination during gastrulation in *Drosophila* embryos. In studies such as these, imaging volumes were limited to a subsection of the *Drosophila* embryo as the biological questions did not require whole embryo information. Studies that require rapid image acquisition, e.g. requiring whole-embryo imaging or monitoring highly dynamic processes, can turn to a faster form of confocal microscopy known as spinning disk.

Spinning disk confocal microscopy improves the image acquisition rate by scanning multiple points simultaneously (**Figure 1**). Yet, there is still an issue of pinhole cross-talk that limits its use with highly scattering specimens. Recently, Shimozawa et al. (13) took a step in addressing these issues with spinning disk by eliminating pinhole cross-talk. Shimozawa and colleagues used a combination of increasing the inter-pinhole distance, and incorporating two-photon illumination in order to improve the spatial resolution attained during spinning disk confocal microscopy.

Confocal microscopy is a widely available, and powerful tool for optical sectioning and imaging deep within highly scattering tissues. Furthermore, because of standard mounting methods (i.e. cover glass mounts), confocal microscopy is currently compatible with microfluidic technology (**Figure 1**), a key tool for integrated approaches aimed at high-content and high-throughput experimentation, which we will cover in subsequent sections. However, there are still drawbacks that limit its use. Specifically, image

acquisition is a time consuming process when compared to epifluorescence microscopy. In addition, whole specimen illumination has the potential for photobleaching, and eliciting phototoxic affects that can negatively impact the development of live embryos and larvae during long-term imaging studies. A microscopy method that addresses these issues is light-sheet microscopy.

2.2. Light-sheet microscopy

Light-sheet microscopy, while established over 100 years ago (14), is experiencing a revival recently with the ability to perform fluorescence light-sheet microscopy, and finding widespread use in studies of development (15-17). Much like confocal microscopy, light-sheet microscopy is an optical sectioning technique that produces higher resolution images than epifluorescence microscopy and allows imaging deep within highly scattering tissues. Although the spatial resolution achieved via light-sheet microscopy is similar to that achieved with confocal, light-sheet offers many advantages over confocal microscopy. Light-sheet microscopy achieves optical sectioning by only illuminating specimens in the focal plane through the use of a "light-sheet" and then detecting the image 90º to the illumination axis (**Figure 1**). In this manner, a single image can be acquired like epifluorescence microscopy when using a real light-sheet, and whole volumes are obtained by moving the specimen through the light-sheet. As a result, image acquisition is much faster in light-sheet microscopy than confocal, while also limiting light exposure to a small section of the specimen at a time, which is ideal for long-term live imaging.

Recent breakthroughs in light-sheet microscopy are improving the capabilities of these microscopes. In 2011, Truong et al. (18) combined light-sheet microscopy with non-linear excitation for improved optical sectioning and increasing the imaging depth by

twofold when compared with single-photon excitation. To similarly improve the spatial resolution achieved by light-sheet microscopy, Keller et al. (19) developed a digitally-scanned light-sheet microscope that can incorporate structured illumination. This allowed Keller and colleagues to image the majority of cellular movements in developing *Drosophila* and zebrafish embryos. However, complete lineage tracing was not possible as image acquisition time exceeded the requisite 30 second imaging frequency to successfully track fast moving cells during development. Further development of the technique by Tomer et al. (20) and Krzic et al. (21) showed that the use of two detection arms in light-sheet microscopy can vastly improve imaging rates. These methods enabled whole-embryo, *in toto* imaging with high enough temporal resolution to allow individual cell tracking throughout *Drosophila* embryogenesis. Long-term imaging up to 20 hours was enabled by minimal photodamage imparted by these imaging methods on developing embryos.

While the in-plane spatial resolution of the aforementioned microscopes are sub-micron, there is still a resolution deficit along the imaging axis (z-direction) of these microscopes. Limited axial resolution in light-sheet microscopy is a result of sparse sampling and the relatively thick shape of conventional light-sheets in the z-direction (i.e. on the order of 5 μm). This is related to the fact that light-sheet microscopes employ Gaussian beams. Ultra-thin light-sheets of less than 0.5 μm are now possible through the incorporation of Bessel beams, which was first introduced by Planchon et al. (22). This allowed Planchon et al. to perform what they termed isotropic imaging as the axial resolution approached ~0.3 μm while imaging single living cells. A limiting factor to this microscope, however, was the fact that the scanning of the Bessel beam to form the light-sheet limited the maximum allowable imaging rates. To improve upon this, Chen et al. (23)

developed lattice light-sheet microscopy, which creates an optical lattice that essentially forms an array of Bessel beams that interact with one another and when dithered form a rapid scanning light-sheet. This microscope allowed Chen et al. to perform 4D super-resolution microscopy with high enough spatiotemporal resolution to track fast, nanoscale processes in living organisms that would otherwise be impossible to track.

Fluorescence light-sheet microscopy has recently become commercially available through the development of systems such as the Lightsheet Z.1 platform developed by Carl Zeiss, and the OpenSPIM platform developed by Pitrone et al. (24). Developments such as these will enable widespread use of this these microscopy techniques in development and biology and general. With the ability to produce massive amounts of bioimage data, i.e. 10s of Terabytes and above, rapid microscopy techniques will ultimately place the bottleneck to research on image processing and data extraction.

3. MICROFLUIDICS AND AUTOMATION FOR MANIPULATING MODELS OF DEVELOPMENT

The use of microfluidic systems in studying biological phenomena has been expanding in recent years, and has been the subject of several reviews (25-27). These systems offer advantages such as parallelized experimentation and integration of automation tools for high-throughput experimentation. In addition, microfluidic systems can be the enabling technology that allows scientists to perform otherwise impossible experiments to address questions in biology that were difficult to answer. Microfluidic-enabled experimentation requires integration of software tools in order to: 1) automate microfluidic operation, and 2) automate data mining and extraction methods. Here, we will review some of the recent

advances made in microfluidic and automation systems used for studying development in multicellular organisms including *Drosophila*, zebrafish, *C. elegans*, mouse, 3D cell culture, and plants.

3.1. *Drosophila*

The fruit fly *Drosophila melanogaster* is a commonly used model of development and behavior, and as such has been subject of previous reviews (28; 29). *Drosophila* is highly accessible genetically, which allows laboratories to house flies with virtually any gene mutant, knock-out, or reporter fusions making genotype-phenotype studies readily available. Furthermore, fruit flies exhibit a short developmental period (i.e. ~24 hours for embryogenesis, and ~10 days from fertilized egg to adult fly), which enables rapid and large-scale developmental studies that are extremely difficult in slower developing organisms such as mice. However, *Drosophila* can be difficult to handle for tasks such as imaging development and behavior, sorting, and microinjection. To address these limitations, several engineered microsystems have been developed to facilitate and automate tedious tasks that often limit experimental throughput. In addition, microfluidic devices have been developed to control the microenvironment in order to spatially (i.e. across individual animals) and temporally perturb development. Here, we will review some of the recent advances made in microfluidic systems used for studying *Drosophila* embryo and larvae development.

3.1.1. *Drosophila* embryos

Drosophila embryos are one of the most experimentally accessible models of embryogenesis, because fertilized embryos are deposited and develop in the environment. While accessing *Drosophila* embryos is easy, manipulating and preparing embryos for

imaging is experimentally difficult. This is because *Drosophila* embryos are relatively small ellipsoids of approximately 200 x 200 x 500 μm, and conventional methods for handling embryos involve time-consuming manual manipulations. Engineered microfluidics systems have been developed to aid in tasks such as embryo sorting (30; 31), microinjection (32), arraying (33-35), and enabling experimental designs involving the spatiotemporal perturbation of embryo development by altering temperature locally to sections of the embryo (36-38), or concentration of chemical species such as methylmercury chloride (39), or oxygen around developing embryos (40).

3.1.1.1. Microfluidic sorting of *Drosophila* embryos

Drosophila is an excellent model for understanding molecular mechanisms of genetic networks, because of *Drosophila*'s fully mapped genome, and genetic accessibility (41). There are many essential genes, an estimated 3600 (42), that if knocked-out cause premature death. In studies aimed at understanding the molecular mechanisms of essential genes, geneticists utilize mutant strains, but the difficulty lies in sorting the 25% homozygous mutants from the rest of the population. Conventional methods require scientists to manually identify embryos of interest and manually isolate them from the rest of the population, which is a time-consuming process. To facilitate this process, Furlong et al. (30) developed a system similar to flow cytometers, which could sort fluorescently-labeled *Drosophila* embryos. This system operates by using fluidics to distribute embryos along a flow path, so that a single embryo will pass through a fluorescence-based detector and sort embryos based on the absence or presence of fluorescence. In this case, Furlong and colleagues employed a magnetically driven valve that would open and close the fluid stream leading to a waste bin. When open, embryos would be sorted to "waste", and when

closed embryos would be sorted to "save". The system engineered by Furlong et al. could automatically sort ~15 embryos per second requiring only pipetting of an embryo suspension to the inlet of the device. Today, there are commercially available systems produced by Union Biometrica, known as the Complex Parametric Analyser and Sorter (COPAS) that can be used to sort particles of up to 1,500 μm in diameter allowing its use with sorting *Drosophila* and zebrafish embryos. This system uses absence or presence of fluorescence to sort objects as well, but instead of using a magnetic valve, these systems use an air stream to blow away unwanted embryos before delivery to a multiwell plate. The COPAS system is an example of microfluidic technology that can be commercialized and implemented by other laboratories for high-throughput sorting.

3.1.1.2. Microfluidics-assisted microinjection of *Drosophila* embryos

Microinjection is another powerful technique used for the delivery of small molecules such as RNAi into developing embryos; yet it is technically challenging due to tedious hand manipulations required for conventional microinjection. Delubac et al. (32) constructed a microfluidic system with an integrated microinjector for automated microinjection of *Drosophila* embryos. The microfluidic device would automatically retrieve embryos from a reservoir, and deliver embryos to the microinjector by sheath flow. Embryos are punctured with a microneedle by flowing embryos into the microinjector rather than moving the injector into the embryo. A camera at the injection site automatically detects the presence of an embryo, sends a command to the microinjector for injection, and following injection the embryo is unloaded to a collection reservoir solely by fluid flow. Delubac et al. showed the viability of the system by injecting eGFP-expressing embryos with siRNA against eGFP. In this setup, Delubac et al. could inject one embryo every 3-4

seconds (231 injected embryos after 14 minutes) with 90% successful silencing of GFP fluorescence.

3.1.1.3. Microfluidic arraying of *Drosophila* embryos for imaging

Dorsal-ventral patterning in *Drosophila* is one of the most well-understood and studied genetic networks, but is experimentally difficult to study due to tedious manual manipulation required for end-on imaging. Witzberger *et al.* (43) used confocal microscopy in conjunction with a custom built imaging slide to directly image ventral furrow formation in live *Drosophila* embryos via end-on imaging. The slide consisted of a fabricated well array, in which embryos were placed on either anterior or posterior pole (**Figure 2**). However, this method is technically challenging because it involves the manual placement of embryos into each well. Chung et al. (33; 34) developed a microfluidic embryo trap array that can automatically orient both live and fixed embryos for end-on imaging through the use of passive hydrodynamics (**Figure 2**). This system allowed orienting of several hundreds of embryos in a matter of minutes, and quantitatively established the dorsal-ventral extents of genes involved in dorsal-ventral patterning. Levario et al. (40) developed a platform that integrates microfluidics, automated image processing and data extraction to quantitatively study the developmental response of *Drosophila* embryos to brief anoxia. This platform utilized an optimized microfluidic device for arraying 10s of live embryos, and used the microfluidic channels to deliver brief pulses of anoxia to developing embryos. Using this system, Levario and colleagues were able to quantitatively measure anoxia-induced developmental delay and response kinetics. A similar microfluidic device was developed by Levario et al. (35) for automatic arraying of live *Drosophila* embryos with a lateral orientation for longitudinal studies of embryogenesis. All of the microfluidic arrays

described here do not require the use of chemicals for immobilizing embryos, and immobilization is simply achieved by physical confinement within microfluidic traps, thus eliminating potentially harmful chemical effects. An in depth discussion about the use of the microfluidic embryo trap array and quantitatively studying the dorsal-ventral patterning system is found below as a case study.

3.1.1.4. Microfluidic-enabled spatiotemporal perturbation of *Drosophila* embryogenesis

One of the biggest advantages to utilizing microfluidics is the ability to perform experiments that are extremely difficult, or simply not possible without microfluidic technology. As mentioned above, Levario et al. used a microfluidic array to temporally expose live *Drosophila* embryos to anoxia, and continuously monitor the developmental responses *in vivo* during end-on imaging. Although manual manipulation to carry out this experiment may be possible, difficulties associated with stably orienting embryos with glue for end-on imaging and maintaining end-on orientation while blowing nitrogen gas over embryos would lead to low success rates and low-throughput that would make this an unattractive approach to such an experiment. In addition, the microfluidics approach can allow a precise control of timing and duration of exposure as well as the spatial patterns of the microenvironment.

Spatially controlling the microenvironment is enabled by physical phenomena that occur at the micron-scale. Fluid flow in micrometer-sized channels is characterized by laminar flow fields as indicated by low Reynold's Number. Laminar flow is described as fluid particles moving in "sheets" next to one another and exhibiting no convective mixing (**Figure 3A**). That means only diffusion exists along the axis perpendicular to the flow direction. Operating microfluidic devices with high Péclet Number (i.e. the ratio of

convective mass/heat transport to diffusive mass/heat transport) allows stable step-changes and stable gradients in concentration or temperature to exist across microfluidic channels. Lucchetta et al. (36) developed a microfluidic device that can impose a temperature step-change across a single embryo (**Figure 3B**), and found that embryos develop normally when anterior/posterior halves grow at different temperatures. The results suggested that in face of environmental perturbations, a simple reciprocal gradient system is not the mechanism for developmental robustness in anterior-posterior patterning. Lucchetta et al. (38) further used this experimental setup with a *Drosophila* strain expressing a Bicoid-GFP (Bcd) fusion and showed that a precise Bcd gradient is not necessary for normal development. In addition, it is suggested that a simple diffusion-established Bcd gradient could not account for robust anterior-posterior patterning. One of challenges associated with the system developed by Lucchetta et al. (36) is the manual mounting of single embryos within the microfluidic device. Dagani et al. (37) incorporated microfluidic self-assembly in order to eliminate tedious hand placement of embryos within the microfluidic channel.

3.1.1.5. Microfluidic integration with light-sheet

One of the greatest challenges for microfluidic technologies is integration with light-sheet microscopy. Microfluidic devices commonly employ glass cover slips for the imaging side of the device, which would cause significant optical aberrations during light-sheet microscopy. Recently, McGorty et al. (39) developed an open-top selective plane illumination compatible microfluidic device, one of the first of its kind. The key to this breakthrough was the fabrication of a water prism that reduces optical aberrations that are caused by imaging through a glass cover slip at 45^{o}. McGorty and colleagues were able to

construct this water prism on the bottom sides of multiwell plates as well as microfluidic devices, which enabled imaging of *Drosophila* embryos and larvae, adult *C. elegans*, and zebrafish embryos with inverted selective plane illumination. Combining the water prism with a microfluidic gradient generator allowed McGorty et al. to expose developing embryos to different concentrations of methylmercury chloride, and continuously image several embryos in parallel throughout development via selective plane illumination.

3.1.2. Microfluidics for immobilizing and imaging *Drosophila* larvae

Drosophila larvae are great models of development as well as neuroscience owing to the fairly transparent appearance of the larvae, which allows direct imaging of biological processes. However, one of the biggest challenges associated with imaging *Drosophila* larvae is immobilization. Conventional methods use either glue or anesthetics to prevent larval locomotion (44), both of which have the potential to negatively affect biological processes under investigation. Many research groups have developed microfluidic systems for physically confining *Drosophila* larvae for imaging unanesthetized animals. Yan et al. (45) constructed a microfluidic device that can *Drosophila* larvae through the action of a mechanical microcompressor. Integration of microfabricated glass channels allows fluidic access to specimens enabling on-chip perfusion during imaging. Using this system with two-photon confocal microscopy allowed Yan and colleagues to image E-cadherin dynamics in the eye imaginal disc in a live third instar larvae expressing an E-cadherin-GFP fusion.

Incorporation of genetically-encoded calcium indicators with these microfluidic devices enables chemical-free imaging of neuronal activity. Ghaemi et al. (46) constructed two microfluidic devices, to immobilize third instar larvae expressing a pan-neuronal

calcium indicator. Using these devices, Ghaemi and colleagues monitored neuronal responses to auditory stimuli and found that neuronal responses peak at 200 Hz. Ghannad-Rezai et al. (47) developed two microfluidic chips for short-term imaging experiments (up to 1 hour), and long-term imaging experiments (up to 10 hours). Using these devices, Ghannad-Rezai and colleagues investigated the short-term and long-term *in vivo* cellular responses to neural injury. Mondal et al. (48) developed a microfluidic device for immobilizing *Drosophila* larvae expressing fluorescently-labeled mitochondria, and were able to monitor mitochondrial transport in unanesthetized animals. The advantages of using microfluidic devices with *Drosophila* larvae, as illustrated by the above systems, are elimination of time-consuming manual manipulation, and enabling chemical-free immobilization and imaging.

3.2. Zebrafish

Zebrafish embryos and larvae are other common models of developmental biology, and besides fundamental studies are extensively used in the fields of drug discovery, molecular toxicity, and therapeutics (49; 50). Zebrafish are fairly simple vertebrates with transparent appearance making it possible to directly image developmental processes *in vivo*. The ability to image individual embryos throughout time is an important requirement for longitudinal studies such as drug discovery, and generally involves physical segregation of embryos using multiwell plates to track individuals across time. Consequently, these types of studies suffer from conventional, low-throughput liquid handling techniques such as manual pipetting and serial dilution. To address these issues several groups have developed microfluidic devices to chemically perturb zebrafish embryos with drugs (51-56), ethanol (57), hypoxia (58), and anti-angiogenics (59; 60); as well as devices for monitoring whole-

brain activity (61), metabolic activity (62; 63), phenotyping (64), and studying mechanical effects on embryo development (65).

3.2.1. Microfluidic arrays for studying zebrafish embryos and larvae

One of the most common microfluidic designs for manipulating model organisms as well as zebrafish embryos and larvae are microfluidic arrays (51-57; 59; 60; 62; 63). Similar to conventional array formats (e.g. multiwell plates), microfluidic arrays allow scientists to parallelize experimentation and data collection from many specimen simultaneously, while also offering spatial registration to track individuals throughout time. However, the advantage of utilizing microfluidic arrays is the ability to automate several processes. For example, microfluidic arrays can enable automated perfusion of the microenvironment obviating conventional liquid handling tasks that involve time-consuming, manual pipetting. Furthermore, microfluidic arrays offer the ability to customize experimental setups and integrate modules such as gradient generators (51; 52; 55; 56), temperature control (66), or on-chip chemical sensors (62; 63) for increased functionality. The primary goal in engineering microfluidic array formats is to arrive at fully automated systems that enable unsupervised experimentation and data collection. Such a system requires the integration of microfluidic technology as well as automation software, which is a characteristic for many of these engineered microfluidic platforms.

3.2.2. Microfluidics for specialized applications involving zebrafish

Microfluidic devices can be engineered for specific applications to address questions that are difficult or even impossible to answer without microfluidic technology. For example, Behrendt et al. (65) fabricated an agarose-based tube to mechanically deform zebrafish embryos in order to show that cable-constriction motors are not essential for epiboly

movements during zebrafish embryogenesis, and that flow-friction motors are sufficient to drive this process. Erickstad et al. (58) developed a microfluidic device that can immobilize unanesthetized zebrafish larvae for brightfield imaging, and temporally expose larvae to varying degrees of hypoxia. Lin et al. (61) developed a similar device to chemically perturb zebrafish larvae with various pharmaceuticals, and utilized transgenic lines expressing calcium indicators in order to perform real-time recording of neural activity within the brain and body. More recently, Pardo-Martin et al. (64) developed an integrated system for high-resolution imaging of zebrafish larvae. This utilized a combination of microfluidic manipulation and imaging of zebrafish larvae, and custom built phenotypical classifying algorithms to identify drug-induced phenotypical alterations. This is an example of a successful system, which integrates advanced microscopy, microfluidic-enabled automation, and autonomous data extraction techniques for high-throughput, high-content experimentation.

3.3. *C. elegans*

The nematode *C. elegans* is another widely used model system. *C. elegans* has a fully mapped genome as well as a relatively simple nervous system of 302 neurons and a fully mapped connectome (67; 68). Microfluidic systems have been developed for studies of neural development (69; 70) as well as nerve degeneration and regeneration (71-73), aging (74-77), embryogenesis (78; 79), and screening/sorting applications (80-84).

3.3.1. Microfluidics-enabled rapid phenotyping and sorting

Many successful systems utilize a combination of microfluidics-assisted manipulation and imaging, and custom built software for automated data extraction for rapid phenotyping. Several approaches were developed (71; 72; 80; 81) for high-throughput screening and

sorting of larval and adult *C. elegans*. The advantage in sorting speed is offered by the automated handling of specimens through microfluidic control, and obviates time-consuming manual manipulation. Chung et al. (81) incorporated computer vision tools for automated, real-time phenotyping of adult *C. elegans* synaptic features, which enabled unsupervised screening that could be performed 100x faster than manual screening methods (69) (**Figure 4**). Important to point out here again is the distinction between microfluidic automation software, and data analysis software, both of which are important to the success of these systems.

3.3.2. Microfluidics-assisted laser axotomy

A common technique used in studying nerve regeneration and degeneration is laser axotomy wherein neurons are cut via laser ablation, and subsequent degeneration/regeneration is monitored by *in vivo* live imaging. This technique is time-consuming, because of the difficulty with which it is to orient and immobilize animals for laser microsurgery. Typically, this is aided by anesthetics to immobilize specimen; however, this is not ideal as anesthetics could likely affect the degeneration/regeneration process. Guo et al. (71) developed a microfluidic device to immobilize larvae for on-chip laser axotomy using mechanical restraints, and found that axonal regeneration occurs more rapidly than previously known. Samara et al. (72) utilized a similar microfluidic-enabled, laser axotomy approach in a drug screen to find small molecule enhancers of regeneration. This approach allowed a faster screen than manual methods, and from a library of ~100 molecules identified several chemicals that significantly alter neural regeneration.

3.4. Microfluidic systems for studying other models of developmental biology

In addition to systems constructed for *Drosophila*, zebrafish, and *C. elegans*, there for have been microfluidic devices developed for manipulating other models of development such as mouse embryos (85-90), cell aggregates (91-95), and plants (96). Esteves et al. (89) developed a microfluidic device for *in vitro* culture of pre-implantation mouse embryos that were subsequently transferred *in utero*, and could achieve birth rates comparable to conventional pre-implantation culture methods. Occhetta et al. (95) developed a microfluidic system to form cell aggregates on-chip, culture cell aggregates on-chip, and deliver defined concentrations of morphogens for directed-differentiation on-chip. Busch et al. (96) developed the RootArray, a microfluidic device that could grow 64 *Arabidopsis thaliana* seedlings, and allow time-lapse imaging of root development on-chip. All of the methods outlined above show the wide range of applications that can be addressed with microfluidic technology, and enable high-throughput experimentation across several models of developmental biology.

4. IMAGE ANALYSIS SOFTWARE AND COMPUTER VISION FOR DEVELOPMENTAL BIOLOGY

High-content, high-throughput research in development, and biology in general, depend upon the development of computer software tools for high-throughput data analysis. With advancing fields of fluorescence microscopy and microfluidics-based experimentation, the bottleneck in many cases now shifts to image processing and data extraction. Over the past decade there have been significant developments in the area of open source bioimage processing and analysis software such as Fiji (97), ICY (98), CellProfiler (99), BioImageXD (100), BigDataViewer (101), V3D (102), and CARTA (103) to name a few.

There are several great reviews that focus on software for data visualization in biology that we highly recommend for readers interested in a more in depth review of the subject matter and a more comprehensive list of available software (104-108). An important consideration in data analysis software is generalizability, which refers to the ease with which a particular software can adapt to different applications. Here, we want to focus on bioimage data extraction methods that specifically relate to cell lineaging (109-112), the concept of virtual embryos (113-116), and computer vision-based phenotyping (69; 117-119).

4.1. Automated cell lineaging

A major challenge in developmental biology is the imaging and tracking of all cells in entire developing embryos throughout all of embryogenesis. Part of the problem is related to acquiring 4D imaging data with high enough spatiotemporal resolution to see all cell tracks. The other part of the problem has to do with reconstructing cell tracks throughout development. This is conventionally attained by manual annotation, which is a painstakingly slow process. Bao et al. (111) developed STARRYNITE to analyze 4D confocal imaging data of developing *C. elegans* embryos and construct cell lineage trees up to the 350-cell stage of development in 25 minutes. The invariant cell lineages exhibited in *C. elegans* development allows straightforward identification of the same cell across individuals, and straightforward comparisons of lineage phenotypes. However, this is made more difficult in more complex organisms such as *Drosophila* and zebrafish, which likely exhibit heightened cell lineage variability in addition to the relative increase in embryo size and cell numbers. Recently, Amat et al. (112) developed an open-source computational framework for segmentation and tracking of cell lineages from large-scale fluorescence microscopy images. The generalizability of the software allows analysis of bioimage data

sets of several model organisms (e.g. *Drosophila*, zebrafish, and mouse) acquired from a variety of microscopy techniques including confocal and light-sheet. The software is user-friendly requiring only the adjustment of 2 parameters for analyzing all data sets, which allows this type of software to be easily adopted by other laboratories.

4.2. Virtual embryos

Another challenge for developmental biology is comparing whole-embryo development between individuals. A virtual or digital embryo, which is an idealized, average embryo that can represent all embryos of the same genotype raised in the same environmental condition can be used for this issue (**Figure 5A**). Creating virtual embryos is a challenge in of itself, because of inherent developmental variability exhibited throughout development. Fowlkes et al. (113) constructed a spatiotemporal atlas of gene expression patterns in the *Drosophila* blastoderm, which was built upon a virtual embryo. By creating a virtual embryo, Fowlkes and colleagues could capture average gene expression patterns by removing inter-embryo variations in morphology, and gene expression. The purpose of this method is to establish gene expression networks, and Fowlkes and colleagues showed that they could recover already known gene interactions from the virtualized map, and predict hundreds more. Murray et al. (120) built upon the STARRYNITE software in order to automatically map spatiotemporal gene patterning throughout *C. elegans* embryogenesis, and enabled comparisons between lineage phenotypes. Virtual Brain Explorer (ViBE-Z) was developed by Ronneberger et al. (115) for automated mapping of gene expression patterns observed in zebrafish larval brains, and can automatically identify anatomical locations for registration. One of the main goals of these projects is to enable direct and easy comparison between embryos to uncover the effects of particular genes, drugs, and

environmental conditions on the development of entire embryos. Kobitski et al. (116) constructed a digital zebrafish embryo, and used it to compare the developmental phenotypes between wildtype embryos and mutants. Kobitski and colleagues found that the one-eye pinhead (oep) mutant shows abnormal development several hours prior to any phenotypic alterations can be seen by eye.

4.3. Computer vision for automated phenotyping

Interpretation of bioimage data is conventionally performed by manual inspection (i.e. seen by eye) and sufficient in many cases especially when obvious changes in phenotypes are observed. However, experimental results in developmental biology are often noisy, because of inherent developmental variability across individuals of a population. This makes manual data interpretation difficult. In this area, computer vision can be used to extract useful information from bioimage data and "see" what is not easily seen by eye. For more detailed information regarding computer vision in biology readers can refer to the following reviews (121; 122). Computer vision has been applied to many studies of biology, but has been more extensively used in studies of individual cells and tissues (118; 119; 123). For example, Yin et al. (117) used support vector machines in a RNAi screen for automated classification of cellular phenotypes, and identification of genetic regulators of cell morphology and the cytoskeleton. The application of computer vision-based classification and data analysis to multicellular organisms is more limited, and primarily used for automating cell lineaging as outlined above. Recently, Crane et al. (69) integrated computer vision with microfluidics-based screening to perform autonomous genetic screening for genes involved in synaptogenesis during *C. elegans* development. Crane and colleagues developed a computational platform for image segmentation, feature extraction, and animal

classification based on extracted features (**Figure 5B**). Computer vision is useful in these cases, because tasks such as whole-animal classification can be performed based on non-obvious phenotypic descriptors. Bioimage classification such as this is ubiquitous in imaging-based studies of biology, and as a result computer-vision based analysis should find widespread use in the near future.

5. QUANTITATIVE ANALYSES AND MODELING- A CASE STUDY ON PATTERN FORMATION

Microfluidic devices enable systematic studies of multiple processes in developing embryos. One of the most extensive applications of microfluidic approaches was demonstrated in the quantitative analysis of pattern formation in the early *Drosophila* embryo, a leading system in molecular studies of embryonic development (33; 124-130). The early *Drosophila* embryo is a syncytium, a system in which nuclei divide synchronously in the common cytoplasm. After 13 synchronous divisions, which corresponds to ~2 hours after egg activation, most of the nuclei are arranged in a two-dimensional layer under a common plasma membrane (**Figure 6A**). The 3rd hour of development is marked by dynamic patterning of this spatially uniform arrangement of nuclei. During this time, nonuniform expression patterns are established for hundreds of zygotic genes. To a first approximation, these patterns can be assigned to two broad categories: anteroposterior (AP) and dorsoventral (DV) (**Figure 6B-D**). With a microfluidics device that helps end-on imaging of *Drosophila* embryos, we were able to image DV cross-sections as shown in Figure 7A-D. Here we focus on the DV patterns and

discuss how microfluidics-based studies were used to test the regulatory mechanisms proposed for the emergence of these patterns.

The emergence of the AP and DV patterns reflects the action of maternally provided inductive signals, established by distinct symmetry breaking events during oogenesis. The asymmetries come in two forms: as localized mRNA inside the egg and as localized biochemical modifications of the extracellular matrix surrounding the oocyte (131). The DV patterning system relies on the second type of asymmetry. In this case, signaling events within the developing egg result in the modification of the extracellular matrix side of the oocyte. Upon egg activation, this modification induces the localized production of Spätzle, a ligand that activates the Toll receptors, which are uniformly distributed along the plasma membrane of the embryo. Locally activated Toll signals through the highly conserved NF-κB pathway and leads to the spatially nonuniform nuclear import of Dorsal (Dl), an NF-κB transcription factor that initiates spatially nonuniform gene expression along the DV axis (**Figure 6D, 7B**) (132). Nuclear Dl triggers DV patterning by directly binding to the regulatory regions of these target genes, some of which then go on to work together with Dl to generate patterns of increasing complexity.

The DV patterning system has been studied extensively since the discovery of the graded distribution of nuclear Dl (133-135). These studies led to the core model for the DV patterning network, in which a broad, ventral-to-dorsal, gradient of nuclear Dl serves as an essential input that controls gene expression both directly and through transcriptional and cell signaling cascades. This model was established in studies with mutants with altered levels of Toll signaling, gene reporter assays, transcriptional profiling experiments, and post-genomic approaches, including genome-wide analysis of DNA binding of Dl and its

co-regulators (136; 137). These studies provided a starting point for the formulation of a quantitative model that could explain how a single graded input leads to the formation of dozens of distinct gene expression domains, all of which are established within a very short time window of about one hour. All of these patterns take the shape of ventral, lateral, or dorsal stripes that span a significant fraction of the AP axis of the embryo. Three of these stripes, each equal to ~1/3 of the system size, are shown in **Figure 7C**. Another stripe, with a much narrower width, is shown in **Figure 7D**. Microfluidic array for end-on imaging of *Drosophila* embryos facilitated the visualization of the spatial distribution of the DV patterning genes along the DV axis (124).

What controls the position and widths of different expression domains (**Figure 7E**)? The first set of mechanisms relies of direct transcriptional control by Dl, which can act both as an activator and as a repressor, depending on the composition of the regulatory sequence of a target gene. For instance, the dorsal border of short gastrulation (sog) and ventral border of the expression of zerknullt (zen) almost coincide and are located at ~2/3 of the entire domain (33). Experiments with the transcriptional reporters for these genes strongly suggest that both of these borders reflect their direct control by Dl: direct activation in the case of sog and direct repression in the case of zen (138). These results imply that the Dl gradient is sufficiently long-ranged to directly control its target genes at this point along the DV axis. Is this actually the case? Answering this question requires quantitative information about the dorsal gradient along the entire DV axis. This information has been provided by studies in which dozens of embryos have been oriented vertically in the microfluidic device, enabling statistical analysis of the spatial distribution of nuclear Dl (33). In one of statistical tests, we determined the position at which the mean value of nuclear Dl becomes

indistinguishable from the background level, defined as the value of nuclear Dl at the dorsalmost position in the embryo. Based on this test, this position is located at ~2/3 of the DV axis, which is in close agreement with the value suggested by the expression domains of sog and zen (**Figure 7F**).

In addition to working as a direct regulator of its target genes, Dl controls them through a number of intermediates. For example, direct effects of high levels of nuclear Dl at the ventral side of the embryo induce the expression of Snail (Sna), which represses a number of Dl-target genes. One of these genes is sog, which is broadly induced in the ventral 2/3 of the embryo. In the ventral 1/3 of the embryo, however, sog is repressed by sna, which defines the ventral border of the sog expression pattern (**Figure 7C,G**). A similar mechanism, based on direct activation by Dl and ventral repression by Sna, controls a number of Dl-target genes that are expressed in lateral stripes. The ventral borders of these stripes coincide but the position of the dorsal expression borders varies greatly (**Figure 7E**). What accounts for these gene-to-gene variations in the dorsal expression borders of Dl-target genes?

An early model suggested that these differences can be explained by differences in the number and/or strengths of Dl binding sites within the regulatory regions of different genes activated by Dl (139). The feasibility of this model was demonstrated in experiments in which the number and strength of Dl binding sites was changed within the same regulatory element. Subsequent studies, however, revealed that real mechanisms are combinatorial in nature and depend on the joint of effects of Dl and other transcription factors (126; 140). One of these factors is Zelda (Zld), a Zn-finger transcription factor that plays a key role in the initiation of zygotic gene expression in the embryo (141). Zld is

distributed uniformly within the embryo and controls gene expression by direct and specific binding to regulatory regions of hundreds of genes, some of which are controlled by Dl.

Analysis of the distribution of the Zld binding sites within the enhancers of Dl-target genes along the DV axis led to a revised model for the quantitative control of their expression domains. According to this model, proximally located binding sites for Dl and Zld can lead to cooperative binding of the two factors (**Figure 7H**). As a result, the occupancy of the Dl binding sites in different enhancers is controlled not only by the number and strengths of these sites, but also by the number, strength, and position of the binding sites for Zld (**Figure 7I**). Experimental tests of this model relied on the quantitative analysis of the expression domains of the Dl target genes as well as the expression of the transcriptional reporters with the altered number of Zld binding site (126). It was essential to monitor transcriptional activity throughout the entire DV axis. This was readily accompanied in microfluidic devices with vertically oriented embryos.

The model based on the combinatorial effects of graded and uniform factors made a number of clear predictions. First, the widths of the lateral expression stripes should be significantly reduced in the absence of Zld. This was consistent with the results of previous experimental studies with embryos lacking maternally provided Zld. **Figure 7J** demonstrates this effect for the expression domain of sog, which is contracted in the most dramatic way (126). Second, the model predicts that changing the number of Zld binding sites within enhancers of Dl target genes can change the width of their expression patterns: reducing the expression domain in response to removal of Zld binding sites and expanding the expression domain in response to addition of extra Zld binding sites. This prediction was confirmed experimentally, using enhancers of two genes with different wild type

expression patterns (128). Furthermore, the model predicts that the presence of Zld binding sites within the enhancers of Dl target genes increases their occupancy by Dl. This prediction was also confirmed experimentally (128).

All of the mechanisms described so far were based on transcriptional cascades triggered by a single extracellular input, the activation of the Toll receptors. In these mechanisms, response to the Dl gradient does not depend on additional signals and interactions between cells within the patterned systems. Such mechanisms can account for the formation of relatively broad domains, but a number of Dl-target genes, including the intermediate neuroblasts defective (ind), are more narrow (**Figure 7D**). Genetic studies of the DV system established that, in addition to the purely cell-autonomous transcriptional cascade downstream of Dl, the expression of ind also depends on extracellular signaling mediated by the highly conserved Epidermal Growth Factor Receptor (EGFR) (142). EGFR signals through the extracellular signal regulated kinase (ERK) pathway, which has been implicated in tissue patterning across species, from planaria to mammals (143-145). In most of the studied developmental contexts, ERK is activated by locally produced extracellular ligands and controls gene expression by phosphorylating transcription factors (146).

The same mechanism works during the control of ind. In this case, transcriptional cascade downstream of nuclear Dl leads to the localized expression of rhomboid (rho), which encodes a ligand-releasing protease within the *Drosophila* EGFR pathway. Locally expressed rho controls localized secretion of short-ranged EGFR ligands which activate ERK signaling, leading to the phosphorylation of a transcriptional repressor of ind (147; 148). At the same time, ind is activated by broadly distributed Zld and Dl (**Figure 8A,B**). Transcriptional relief of ind by the ERK pathway is realized in cells expressing rho and

their neighbors, but ind is expressed only on one side of the rho-expression domain, reflecting the effects of ventrally localized repressors (130; 149).

What aspects of ERK signaling are important for ind expression? Is it the amplitude of ERK signaling, its duration, a time integral of ERK activation, etc? Similar questions can be posed for in countless developmental systems patterned by locally activated ERK signals. Surprisingly, the answers to these questions are unknown, mainly because of experimental difficulties with detailed spatiotemporal analysis of ERK signaling in developing tissues. Using microfluidics-based imaging assays, we could provide a clear answer to these questions for the ERK-dependent expression of ind (130). In these experiments, fixed embryos were stained to reveal the spatial distribution of rho and ind mRNA and ERK phosphorylation. These spatial patterns were then ordered in time, using an imaging processing algorithm that matched the morphology of fixed embryos to snapshots from live imaging of morphogenesis (**Figure 8C**). Each of the fixed snapshots of rho, ind, and active ERK could be timed with precision of ~3 minutes, providing an unprecedented view of ERK signaling dynamics in a developing tissue (**Figure 8D**).

Detailed analysis of timed snapshots in both the wild type and mutant embryos revealed that active ERK works as a simple switch: ind is induced after ERK activation crosses a critical threshold. Beyond this threshold dynamics of the ERK pathway appears to be irrelevant. In addition to providing the first high resolution view of developmental dynamics of ERK, this work established a powerful experimental system which can be used to explore how this highly conserved signaling pathway is controlled by multiple components involved in signal transmission downstream of ligand-activated receptor

tyrosine kinases, such as EGFR (130). In our current experiments, we are using microfluidics-based imaging to address this question.

Quantitative analysis of pattern formation by protein gradients requires characterization of the gradients and their effects on target genes in a large number of embryos, at multiple time points, and in multiple mutant backgrounds. Using combinations of microscopy, microfluidics-based imaging, and quantitative image analysis tools, we performed large-scale analysis of the pattern formation in early *Drosophila* embryos. We provided statistical analysis on the spatial range of Dl morphogen gradient and the DV border of its target genes for the first time. We tested direct effects of combinatorial gene regulation between Dl and Zld. Lastly, we were also able to provide the first high resolution view of developmental dynamics of the ERK-mediated ind regulation, which is also indirectly regulated by Dl. Further development of imaging and microfluidics-aided techniques will allow an access to better understanding of the spatial and temporal gene expression patterns and regulatory mechanisms not only in *Drosophila,* but in other organisms as well.

6. CONCLUSION AND OUTLOOK

Integrated approaches that combine advanced microscopy techniques, microfluidic and automation technologies, and computer-vision are vital for the progression of quantitative biology. A key challenge for integrated systems is the combining of fluorescence light-sheet microscopy with microfluidic technologies. Ultimately, this requires an optically uniform imaging axis, because any slight deviation in refractive index between the imaging solution and microfluidic device results in significant optical aberrations. Widespread use

of microfluidic technologies in biology depends on the development of user-friendly device designs as well as user-friendly automation software. Keeping microfluidic devices as simple as possible is key, which determines how simple or complex the automation software will be for operation. High-content imaging and high-throughput experimentation in biology enabled by fluorescence microscopy and microfluidic technologies ultimately place the bottleneck of experimental throughput on data analysis, and requiring incorporation of computer-vision techniques for automated data extraction. Integrated approaches incorporating fluorescence imaging, microfluidics, and computer-vision will enable high-throughput quantitative biology, and widespread adoption of these approaches will be facilitated by the development of simple, user-friendly, and generalizable microfluidic devices, and automation software.

DISCLOSURE STATEMENT

The authors are not aware of any affiliations, memberships, funding, or financial holdings that might be perceived as affecting the objectivity of this review.

ACKNOWLEDGEMENTS

This work was supported by the US National Science Foundation (EFRI 1136913 to S.Y.S. and H.L.), and the US National Institutes of Health (GM078079 to S.Y.S., 1F31AA023160-01 to T.J.L., and GM088333 to H.L.).

LITERATURE CITED

1. Teleman AA, Cohen SM. 2000. Dpp gradient formation in the Drosophila wing imaginal disc. *Cell* 103:971-80
2. Kiehart DP, Galbraith CG, Edwards KA, Rickoll WL, Montague RA. 2000. Multiple forces contribute to cell sheet morphogenesis for dorsal closure in Drosophila. *J Cell Biol* 149:471-90

3. Gong Y, Mo CH, Fraser SE. 2004. Planar cell polarity signalling controls cell division orientation during zebrafish gastrulation. *Nature* 430:689-93
4. Patel MR, Lehrman EK, Poon VY, Crump JG, Zhen M, et al. 2006. Hierarchical assembly of presynaptic components in defined C. elegans synapses. *Nat Neurosci* 9:1488-98
5. Verveer PJ, Swoger J, Pampaloni F, Greger K, Marcello M, Stelzer EHK. 2007. High-resolution three-dimensional imaging of large specimens with light sheet-based microscopy. *Nat Methods* 4:311-3
6. Zanacchi FC, Lavagnino Z, Donnorso MP, Del Bue A, Furia L, et al. 2011. Live-cell 3D super-resolution imaging in thick biological samples. *Nat Methods* 8:1047-+
7. Hagerling R, Pollmann C, Andreas M, Schmidt C, Nurmi H, et al. 2013. A novel multistep mechanism for initial lymphangiogenesis in mouse embryos based on ultramicroscopy. *Embo J* 32:629-44
8. Ahrens MB, Orger MB, Robson DN, Li JM, Keller PJ. 2013. Whole-brain functional imaging at cellular resolution using light-sheet microscopy. *Nat Methods* 10:413-+
9. Reeves GT, Trisnadi N, Truong TV, Nahmad M, Katz S, Stathopoulos A. 2012. Dorsal-Ventral Gene Expression in the Drosophila Embryo Reflects the Dynamics and Precision of the Dorsal Nuclear Gradient. *Dev Cell* 22:544-57
10. Denk W, Strickler JH, Webb WW. 1990. Two-photon laser scanning fluorescence microscopy. *Science* 248:73-6
11. McMahon A, Supatto W, Fraser SE, Stathopoulos A. 2008. Dynamic Analyses of Drosophila Gastrulation Provide Insights into Collective Cell Migration. *Science* 322:1546-50
12. Wang YC, Khan Z, Wieschaus EF. 2013. Distinct Rap1 Activity States Control the Extent of Epithelial Invagination via alpha-Catenin. *Dev Cell* 25:299-309
13. Shimozawa T, Yamagata K, Kondo T, Hayashi S, Shitamukai A, et al. 2013. Improving spinning disk confocal microscopy by preventing pinhole cross-talk for intravital imaging. *P Natl Acad Sci USA* 110:3399-404
14. Zsigmondy R, Alexander J. 1909. *Colloids and the ultramicroscope; a manual of colloid chemistry and ultramicroscopy*. New York,: J. Wiley & Sons; etc. xiii, 245 p. pp.
15. Voie AH, Burns DH, Spelman FA. 1993. Orthogonal-Plane Fluorescence Optical Sectioning - 3-Dimensional Imaging of Macroscopic Biological Specimens. *J Microsc-Oxford* 170:229-36
16. Huisken J, Swoger J, Del Bene F, Wittbrodt J, Stelzer EHK. 2004. Optical sectioning deep inside live embryos by selective plane illumination microscopy. *Science* 305:1007-9
17. Holekamp TF, Turaga D, Holy TE. 2008. Fast three-dimensional fluorescence imaging of activity in neural populations by objective-coupled planar illumination microscopy. *Neuron* 57:661-72
18. Truong TV, Supatto W, Koos DS, Choi JM, Fraser SE. 2011. Deep and fast live imaging with two-photon scanned light-sheet microscopy. *Nat Methods* 8:757-U102
19. Keller PJ, Schmidt AD, Santella A, Khairy K, Bao ZR, et al. 2010. Fast, high-contrast imaging of animal development with scanned light sheet-based structured-illumination microscopy. *Nat Methods* 7:637-U55
20. Tomer R, Khairy K, Amat F, Keller PJ. 2012. Quantitative high-speed imaging of entire developing embryos with simultaneous multiview light-sheet microscopy. *Nat Methods* 9:755-U181
21. Krzic U, Gunther S, Saunders TE, Streichan SJ, Hufnagel L. 2012. Multiview light-sheet microscope for rapid in toto imaging. *Nat Methods* 9:730-U304
22. Planchon TA, Gao L, Milkie DE, Davidson MW, Galbraith JA, et al. 2011. Rapid three-dimensional isotropic imaging of living cells using Bessel beam plane illumination. *Nat Methods* 8:417-U68
23. Chen BC, Legant WR, Wang K, Shao L, Milkie DE, et al. 2014. Lattice light-sheet microscopy: Imaging molecules to embryos at high spatiotemporal resolution. *Science* 346:439-+

24. Pitrone PG, Schindelin J, Stuyvenberg L, Preibisch S, Weber M, et al. 2013. OpenSPIM: an open-access light-sheet microscopy platform. *Nat Methods* 10:598-9
25. Whitesides GM, Ostuni E, Takayama S, Jiang XY, Ingber DE. 2001. Soft lithography in biology and biochemistry. *Annu Rev Biomed Eng* 3:335-73
26. Beebe DJ, Mensing GA, Walker GM. 2002. Physics and applications of microfluidics in biology. *Annu Rev Biomed Eng* 4:261-86
27. El-Ali J, Sorger PK, Jensen KF. 2006. Cells on chips. *Nature* 442:403-11
28. Campos-Ortega JA, Hartenstein V. *The embryonic development of Drosophila melanogaster*. xvii, 405 pages pp.
29. Bate M, Martinez Arias A. *The Development of Drosophila melanogaster*. 2 volumes (x, 1,558 pages) pp.
30. Furlong EEM, Profitt D, Scott MP. 2001. Automated sorting of live transgenic embryos. *Nat Biotechnol* 19:153-6
31. Chen CC, Zappe S, Sahin O, Zhang XJ, Fish M, et al. 2004. Design and operation of a microfluidic sorter for Drosophila embryos. *Sensor Actuat B-Chem* 102:59-66
32. Delubac D, Highley CB, Witzberger-Krajcovic M, Ayoob JC, Furbee EC, et al. 2012. Microfluidic system with integrated microinjector for automated Drosophila embryo injection. *Lab Chip* 12:4911-9
33. Chung K, Kim Y, Kanodia JS, Gong E, Shvartsman SY, Lu H. 2011. A microfluidic array for large-scale ordering and orientation of embryos. *Nat Methods* 8:171-U03
34. Levario TJ, Zhan M, Lim B, Shvartsman SY, Lu H. 2013. Microfluidic trap array for massively parallel imaging of Drosophila embryos. *Nat Protoc* 8:721-36
35. Levario TJ, Zhao C, Shvartsman SY, Lu H. 2015. Microfluidic arraying and high-throughput imaging of laterally oriented Drosophila embryos. *Lab Chip*
36. Lucchetta EM, Lee JH, Fu LA, Patel NH, Ismagilov RF. 2005. Dynamics of Drosophila embryonic patterning network perturbed in space and time using microfluidics. *Nature* 434:1134-8
37. Dagani GT, Monzo K, Fakhoury JR, Chen CC, Sisson JC, Zhang XJ. 2007. Microfluidic self-assembly of live Drosophila embryos for versatile high-throughput analysis of embryonic morphogenesis. *Biomed Microdevices* 9:681-94
38. Lucchetta EM, Vincent ME, Ismagilov RF. 2008. A Precise Bicoid Gradient Is Nonessential during Cycles 11-13 for Precise Patterning in the Drosophila Blastoderm. *Plos One* 3
39. McGorty R, Liu H, Kamiyama D, Dong ZQ, Guo S, Huang B. 2015. Open-top selective plane illumination microscope for conventionally mounted specimens. *Opt Express* 23:16142-53
40. Levario TJ, Zhao C, Shvartsman SY, Lu H. 2015. Large-scale data collection and precise perturbation of live Drosophila embryos via a microfluidic platform. *Development*
41. Adams MD, Celniker SE, Holt RA, Evans CA, Gocayne JD, et al. 2000. The genome sequence of Drosophila melanogaster. *Science* 287:2185-95
42. Spradling AC, Stern D, Beaton A, Rhem EJ, Laverty T, et al. 1999. The Berkeley Drosophila Genome Project gene disruption project: Single P-element insertions mutating 25% of vital drosophila genes. *Genetics* 153:135-77
43. Witzberger MM, Fitzpatrick JAJ, Crowley JC, Minden JS. 2008. End-on Imaging: A New Perspective on Dorsoventral Development in Drosophila Embryos. *Dev Dynam* 237:3252-9
44. Badre NH, Martin ME, Cooper RL. 2005. The physiological and behavioral effects of carbon dioxide on Drosophila melanogaster larvae. *Comp Biochem Phys A* 140:363-76
45. Yan YJ, Jiang LW, Aufderheide KJ, Wright GA, Terekhov A, et al. 2014. A Microfluidic- Enabled Mechanical Microcompressor for the Immobilization of Live Single- and Multi- Cellular Specimens. *Microsc Microanal* 20:141-51

46. Ghaemi R, Rezai P, Iyengar BG, Selvaganapathy PR. 2015. Microfluidic devices for imaging neurological response of Drosophila melanogaster larva to auditory stimulus. *Lab Chip* 15:1116-22
47. Ghannad-Rezaie M, Wang X, Mishra B, Collins C, Chronis N. 2012. Microfluidic Chips for In Vivo Imaging of Cellular Responses to Neural Injury in Drosophila Larvae. *Plos One* 7
48. Mondal S, Ahlawat S, Rau K, Venkataraman V, Koushika SP. 2011. Imaging in vivo Neuronal Transport in Genetic Model Organisms Using Microfluidic Devices. *Traffic* 12:372-85
49. Zon LI, Peterson RT. 2005. In vivo drug discovery in the zebrafish. *Nat Rev Drug Discov* 4:35-44
50. Lieschke GJ, Currie PD. 2007. Animal models of human disease: zebrafish swim into view. *Nat Rev Genet* 8:353-67
51. Yang F, Chen ZG, Pan JB, Li XC, Feng J, Yang H. 2011. An integrated microfluidic array system for evaluating toxicity and teratogenicity of drugs on embryonic zebrafish developmental dynamics. *Biomicrofluidics* 5
52. Choudhury D, van Noort D, Iliescu C, Zheng BX, Poon KL, et al. 2012. Fish and Chips: a microfluidic perfusion platform for monitoring zebrafish development. *Lab Chip* 12:892-900
53. Bischel LL, Mader BR, Green JM, Huttenlocher A, Beebe DJ. 2013. Zebrafish Entrapment By Restriction Array (ZEBRA) device: a low-cost, agarose-free zebrafish mounting technique for automated imaging. *Lab Chip* 13:1732-6
54. Zheng CH, Zhou HW, Liu XX, Pang YH, Zhang B, Huang YY. 2014. Fish in chips: an automated microfluidic device to study drug dynamics in vivo using zebrafish embryos. *Chem Commun* 50:981-4
55. Li YB, Yang F, Chen ZG, Shi LJ, Zhang BB, et al. 2014. Zebrafish on a Chip: A Novel Platform for Real-Time Monitoring of Drug-Induced Developmental Toxicity. *Plos One* 9
56. Li YB, Yang XJ, Chen ZG, Zhang BB, Pan JB, et al. 2015. Comparative toxicity of lead (Pb2+), copper (Cu2+), and mixtures of lead and copper to zebrafish embryos on a microfluidic chip. *Biomicrofluidics* 9
57. Wielhouwer EM, Ali S, Al-Afandi A, Blom MT, Riekerink MBO, et al. 2011. Zebrafish embryo development in a microfluidic flow-through system. *Lab Chip* 11:1815-24
58. Erickstad M, Hale LA, Chalasani SH, Groisman A. 2015. A microfluidic system for studying the behavior of zebrafish larvae under acute hypoxia. *Lab Chip* 15:857-66
59. Akagi J, Khoshmanesh K, Hall CJ, Crosier KE, Crosier PS, et al. 2012. Fish on chips: Automated Microfluidic Living Embryo Arrays. *Procedia Engineer* 47:84-7
60. Akagi J, Zhu F, Hall CJ, Crosier KE, Crosier PS, Wlodkowic D. 2014. Integrated chip-based physiometer for automated fish embryo toxicity biotests in pharmaceutical screening and ecotoxicology. *Cytom Part A* 85A:537-47
61. Lin XD, Wang SQ, Yu XD, Liu ZG, Wang F, et al. 2015. High-throughput mapping of brain-wide activity in awake and drug-responsive vertebrates. *Lab Chip* 15:680-9
62. Huang SH, Huang KS, Yu CH, Gong HY. 2013. Metabolic profile analysis of a single developing zebrafish embryo via monitoring of oxygen consumption rates within a microfluidic device. *Biomicrofluidics* 7
63. Zhu F, Baker D, Skommer J, Sewell M, Wlodkowic D. 2015. Real-Time 2D Visualization of Metabolic Activities in Zebrafish Embryos Using a Microfluidic Technology. *Cytom Part A* 87A:446-50
64. Pardo-Martin C, Allalou A, Medina J, Eimon PM, Wahlby C, Yanik MF. 2013. High-throughput hyperdimensional vertebrate phenotyping. *Nat Commun* 4
65. Behrndt M, Salbreux G, Campinho P, Hauschild R, Oswald F, et al. 2012. Forces Driving Epithelial Spreading in Zebrafish Gastrulation. *Science* 338:257-60

66. Wang KIK, Salcic Z, Yeh J, Akagi J, Zhu F, et al. 2013. Toward embedded laboratory automation for smart lab-on-a-chip embryo arrays. *Biosens Bioelectron* 48:188-96
67. White JG, Southgate E, Thomson JN, Brenner S. 1986. The Structure of the Nervous-System of the Nematode Caenorhabditis-Elegans. *Philos T Roy Soc B* 314:1-340
68. Consortium CeS. 1998. Genome sequence of the nematode C-elegans: A platform for investigating biology. *Science* 282:2012-8
69. Crane MM, Stirman JN, Ou CY, Kurshan PT, Rehg JM, et al. 2012. Autonomous screening of C-elegans identifies genes implicated in synaptogenesis. *Nat Methods* 9:977-+
70. Caceres ID, Valmas N, Hilliard MA, Lu H. 2012. Laterally Orienting C. elegans Using Geometry at Microscale for High-Throughput Visual Screens in Neurodegeneration and Neuronal Development Studies. *Plos One* 7
71. Guo SX, Bourgeois F, Chokshi T, Durr NJ, Hilliard MA, et al. 2008. Femtosecond laser nanoaxotomy lab-on-achip for in vivo nerve regeneration studies. *Nat Methods* 5:531-3
72. Samara C, Rohde CB, Gilleland CL, Norton S, Haggarty SJ, Yanik MF. 2010. Large-scale in vivo femtosecond laser neurosurgery screen reveals small-molecule enhancer of regeneration. *P Natl Acad Sci USA* 107:18342-7
73. Gokce SK, Guo SX, Ghorashian N, Everett WN, Jarrell T, et al. 2014. A Fully Automated Microfluidic Femtosecond Laser Axotomy Platform for Nerve Regeneration Studies in C. elegans. *Plos One* 9
74. Krajniak J, Lu H. 2010. Long-term high-resolution imaging and culture of C. elegans in chip-gel hybrid microfluidic device for developmental studies. *Lab Chip* 10:1862-8
75. Hulme SE, Shevkoplyas SS, McGuigan AP, Apfeld J, Fontana W, Whitesides GM. 2010. Lifespan-on-a-chip: microfluidic chambers for performing lifelong observation of C. elegans. *Lab Chip* 10:589-97
76. Nghe P, Boulineau S, Gude S, Recouvreux P, van Zon JS, Tans SJ. 2013. Microfabricated Polyacrylamide Devices for the Controlled Culture of Growing Cells and Developing Organisms. *Plos One* 8
77. Yu CC, Raizen DM, Fang-Yen C. 2014. Multi-well imaging of development and behavior in Caenorhabditis elegans. *J Neurosci Meth* 223:35-9
78. Khoshmanesh K, Kiss N, Nahavandi S, Evans CW, Cooper JM, et al. 2011. Trapping and imaging of micron-sized embryos using dielectrophoresis. *Electrophoresis* 32:3129-32
79. Cornaglia M, Mouchiroud L, Marette A, Narasimhan S, Lehnert T, et al. 2015. An automated microfluidic platform for C-elegans embryo arraying, phenotyping, and long-term live imaging. *Sci Rep-Uk* 5
80. Rohde CB, Zeng F, Gonzalez-Rubio R, Angel M, Yanik MF. 2007. Microfluidic system for on-chip high-throughput whole-animal sorting and screening at subcellular resolution. *P Natl Acad Sci USA* 104:13891-5
81. Chung KH, Crane MM, Lu H. 2008. Automated on-chip rapid microscopy, phenotyping and sorting of C. elegans. *Nat Methods* 5:637-43
82. Ai XN, Zhuo WP, Liang QL, McGrath PT, Lu H. 2014. A high-throughput device for size based separation of C-elegans developmental stages. *Lab Chip* 14:1746-52
83. Aubry G, Zhan M, Lu H. 2015. Hydrogel-droplet microfluidic platform for high-resolution imaging and sorting of early larval Caenorhabditis elegans. *Lab Chip* 15:1424-31
84. Wen H, Yu Y, Zhu GL, Jiang L, Qin JH. 2015. A droplet microchip with substance exchange capability for the developmental study of C-elegans. *Lab Chip* 15:1905-11
85. Huang HY, Shen HH, Tien CH, Li CJ, Fan SK, et al. 2015. Digital Microfluidic Dynamic Culture of Mammalian Embryos on an Electrowetting on Dielectric (EWOD) Chip. *Plos One* 10

86. Pyne DG, Liu J, Abdelgawad M, Sun Y. 2014. Digital Microfluidic Processing of Mammalian Embryos for Vitrification. *Plos One* 9
87. Lai D, Ding J, Smith GW, Smith GD, Takayama S. 2015. Slow and steady cell shrinkage reduces osmotic stress in bovine and murine oocyte and zygote vitrification. *Human reproduction* 30:37-45
88. Heo YS, Cabrera LM, Bormann CL, Shah CT, Takayama S, Smith GD. 2010. Dynamic microfunnel culture enhances mouse embryo development and pregnancy rates. *Human reproduction* 25:613-22
89. Esteves TC, van Rossem F, Nordhoff V, Schlatt S, Boiani M, Le Gac S. 2013. A microfluidic system supports single mouse embryo culture leading to full-term development. *Rsc Adv* 3:26451-8
90. Chung YH, Hsiao YH, Kao WL, Hsu CH, Yao DJ, Chen CC. 2015. Microwells support high-resolution time-lapse imaging and development of preimplanted mouse embryos. *Biomicrofluidics* 9
91. Moon SH, Ju J, Park SJ, Bae D, Chung HM, Lee SH. 2014. Optimizing human embryonic stem cells differentiation efficiency by screening size-tunable homogenous embryoid bodies. *Biomaterials* 35:5987-97
92. Wilson JL, Suri S, Singh A, Rivet CA, Lu H, McDevitt TC. 2014. Single-cell analysis of embryoid body heterogeneity using microfluidic trapping array. *Biomed Microdevices* 16:79-90
93. Au SH, Chamberlain MD, Mahesh S, Sefton MV, Wheeler AR. 2014. Hepatic organoids for microfluidic drug screening. *Lab Chip* 14:3290-9
94. Jeong GS, Song JH, Kang AR, Jun Y, Kim JH, et al. 2013. Surface Tension-Mediated, Concave-Microwell Arrays for Large-Scale, Simultaneous Production of Homogeneously Sized Embryoid Bodies. *Adv Healthc Mater* 2:119-25
95. Occhetta P, Centola M, Tonnarelli B, Redaelli A, Martin I, Rasponi M. 2015. High-Throughput Microfluidic Platform for 3D Cultures of Mesenchymal Stem Cells, Towards Engineering Developmental Processes. *Sci Rep-Uk* 5
96. Busch W, Moore BT, Martsberger B, Mace DL, Twigg RW, et al. 2012. A microfluidic device and computational platform for high-throughput live imaging of gene expression. *Nat Methods* 9:1101-+
97. Schindelin J, Arganda-Carreras I, Frise E, Kaynig V, Longair M, et al. 2012. Fiji: an open-source platform for biological-image analysis. *Nat Methods* 9:676-82
98. de Chaumont F, Dallongeville S, Chenouard N, Herve N, Pop S, et al. 2012. Icy: an open bioimage informatics platform for extended reproducible research. *Nat Methods* 9:690-6
99. Carpenter AE, Jones TR, Lamprecht MR, Clarke C, Kang IH, et al. 2006. CellProfiler: image analysis software for identifying and quantifying cell phenotypes. *Genome Biol* 7
100. Kankaanpaa P, Paavolainen L, Tiitta S, Karjalainen M, Paivarinne J, et al. 2012. BioImageXD: an open, general-purpose and high-throughput image-processing platform. *Nat Methods* 9:683-9
101. Pietzsch T, Saalfeld S, Preibisch S, Tomancak P. 2015. BigDataViewer: visualization and processing for large image data sets. *Nat Methods* 12:481-3
102. Peng HC, Ruan ZC, Long FH, Simpson JH, Myers EW. 2010. V3D enables real-time 3D visualization and quantitative analysis of large-scale biological image data sets. *Nat Biotechnol* 28:348-U75
103. Kutsuna N, Higaki T, Matsunaga S, Otsuki T, Yamaguchi M, et al. 2012. Active learning framework with iterative clustering for bioimage classification. *Nat Commun* 3
104. Walter T, Shattuck DW, Baldock R, Bastin ME, Carpenter AE, et al. 2010. Visualization of image data from cells to organisms. *Nat Methods* 7:S26-S41
105. Luengo-Oroz MA, Ledesma-Carbayo MJ, Peyrieras N, Santos A. 2011. Image analysis for understanding embryo development: a bridge from microscopy to biological insights. *Curr Opin Genet Dev* 21:630-7

106. Eliceiri KW, Berthold MR, Goldberg IG, Ibanez L, Manjunath BS, et al. 2012. Biological imaging software tools. *Nat Methods* 9:697-710
107. Hamilton NA. 2012. Open Source Tools for Fluorescent Imaging. *Method Enzymol* 504:393-417
108. Jug F, Pietzsch T, Preibisch S, Tomancak P. 2014. Bioimage Informatics in the context of Drosophila research. *Methods* 68:60-73
109. Khan Z, Wang YC, Wieschaus EF, Kaschube M. 2014. Quantitative 4D analyses of epithelial folding during Drosophila gastrulation. *Development* 141:2895-900
110. Peng HC, Long FF, Zhou J, Leung G, Eisen MB, Myers EW. 2007. Automatic image analysis for gene expression patterns of fly embryos. *Bmc Cell Biol* 8
111. Bao ZR, Murray JI, Boyle T, Ooi SL, Sandel MJ, Waterston RH. 2006. Automated cell lineage tracing in Caenorhabditis elegans. *P Natl Acad Sci USA* 103:2707-12
112. Amat F, Lemon W, Mossing DP, McDole K, Wan Y, et al. 2014. Fast, accurate reconstruction of cell Lineages from Large-scale fluorescence microscopy data. *Nat Methods* 11:951-8
113. Fowlkes CC, Luengo Hendriks CL, Keranen SVE, Weber GH, Rubel O, et al. 2008. A quantitative spatiotemporal atlas of gene expression in the Drosophila blastoderm. *Cell* 133:364-74
114. Fowlkes CC, Eckenrode KB, Bragdon MD, Meyer M, Wunderlich Z, et al. 2011. A Conserved Developmental Patterning Network Produces Quantitatively Different Output in Multiple Species of Drosophila. *Plos Genet* 7
115. Ronneberger O, Liu K, Rath M, Ruess D, Mueller T, et al. 2012. ViBE-Z: a framework for 3D virtual colocalization analysis in zebrafish larval brains. *Nat Methods* 9:735-U316
116. Kobitski AY, Otte JC, Takamiya M, Schafer B, Mertes J, et al. 2015. An ensemble-averaged, cell density-based digital model of zebrafish embryo development derived from light-sheet microscopy data with single-cell resolution. *Sci Rep-Uk* 5
117. Yin Z, Sadok A, Sailem H, McCarthy A, Xia XF, et al. 2013. A screen for morphological complexity identifies regulators of switch-like transitions between discrete cell shapes. *Nat Cell Biol* 15:860-+
118. Collinet C, Stoter M, Bradshaw CR, Samusik N, Rink JC, et al. 2010. Systems survey of endocytosis by multiparametric image analysis. *Nature* 464:243-U123
119. Liberali P, Snijder B, Pelkmans L. 2014. A Hierarchical Map of Regulatory Genetic Interactions in Membrane Trafficking. *Cell* 157:1473-87
120. Murray JI, Bao Z, Boyle TJ, Boeck ME, Mericle BL, et al. 2008. Automated analysis of embryonic gene expression with cellular resolution in C-elegans. *Nat Methods* 5:703-9
121. Danuser G. 2011. Computer Vision in Cell Biology. *Cell* 147:973-8
122. Sommer C, Gerlich DW. 2013. Machine learning in cell biology - teaching computers to recognize phenotypes. *J Cell Sci* 126:5529-39
123. Zhong Q, Busetto AG, Fededa JP, Buhmann JM, Gerlich DW. 2012. Unsupervised modeling of cell morphology dynamics for time-lapse microscopy. *Nat Methods* 9:711-U267
124. Kim Y, Andreu MJ, Lim B, Chung K, Terayama M, et al. 2011. Gene Regulation by MAPK Substrate Competition. *Dev Cell* 20:880-7
125. Helman A, Lim B, Andreu MJ, Kim Y, Shestkin T, et al. 2012. RTK signaling modulates the Dorsal gradient. *Development* 139:3032-9
126. Kanodia JS, Liang HL, Kim Y, Lim B, Zhan M, et al. 2012. Pattern formation by graded and uniform signals in the early Drosophila embryo. *Biophys J* 102:427-33
127. Lim B, Samper N, Lu H, Rushlow C, Jimenez G, Shvartsman SY. 2013. Kinetics of gene derepression by ERK signaling. *Proc Natl Acad Sci U S A* 110:10330-5
128. Foo SM, Sun Y, Lim B, Ziukaite R, O'Brien K, et al. 2014. Zelda potentiates morphogen activity by increasing chromatin accessibility. *Curr Biol* 24:1341-6

129. Dsilva CJ, Lim B, Lu H, Singer A, Kevrekidis IG, Shvartsman SY. 2015. Temporal ordering and registration of images in studies of developmental dynamics. *Development* 142:1717-24
130. Lim B, Dsilva CJ, Levario TJ, Lu H, Schupbach T, et al. 2015. Dynamics of Inductive ERK Signaling in the Drosophila Embryo. *Curr Biol* 25:1784-90
131. Roth S, Lynch JA. 2009. Symmetry breaking during Drosophila oogenesis. *Cold Spring Harb Perspect Biol* 1:a001891
132. Moussian B, Roth S. 2005. Dorsoventral axis formation in the Drosophila embryo--shaping and transducing a morphogen gradient. *Curr Biol* 15:R887-99
133. Rushlow CA, Han K, Manley JL, Levine M. 1989. The graded distribution of the dorsal morphogen is initiated by selective nuclear transport in Drosophila. *Cell* 59:1165-77
134. Steward R. 1989. Relocalization of the dorsal protein from the cytoplasm to the nucleus correlates with its function. *Cell* 59:1179-88
135. Roth S, Stein D, Nusslein-Volhard C. 1989. A gradient of nuclear localization of the dorsal protein determines dorsoventral pattern in the Drosophila embryo. *Cell* 59:1189-202
136. Markstein M, Zinzen R, Markstein P, Yee KP, Erives A, et al. 2004. A regulatory code for neurogenic gene expression in the Drosophila embryo. *Development* 131:2387-94
137. Stathopoulos A, Van Drenth M, Erives A, Markstein M, Levine M. 2002. Whole-genome analysis of dorsal-ventral patterning in the Drosophila embryo. *Cell* 111:687-701
138. Markstein M, Markstein P, Markstein V, Levine MS. 2002. Genome-wide analysis of clustered Dorsal binding sites identifies putative target genes in the Drosophila embryo. *Proc Natl Acad Sci U S A* 99:763-8
139. Papatsenko D, Levine M. 2005. Quantitative analysis of binding motifs mediating diverse spatial readouts of the Dorsal gradient in the Drosophila embryo. *Proc Natl Acad Sci U S A* 102:4966-71
140. Liang HL, Nien CY, Liu HY, Metzstein MM, Kirov N, Rushlow C. 2008. The zinc-finger protein Zelda is a key activator of the early zygotic genome in Drosophila. *Nature* 456:400-3
141. Nien CY, Liang HL, Butcher S, Sun Y, Fu S, et al. 2011. Temporal coordination of gene networks by Zelda in the early Drosophila embryo. *PLoS Genet* 7:e1002339
142. Skeath JB. 1998. The Drosophila EGF receptor controls the formation and specification of neuroblasts along the dorsal-ventral axis of the Drosophila embryo. *Development* 125:3301-12
143. Moghal N, Sternberg PW. 2003. The epidermal growth factor system in Caenorhabditis elegans. *Exp Cell Res* 284:150-9
144. Budi EH, Patterson LB, Parichy DM. 2008. Embryonic requirements for ErbB signaling in neural crest development and adult pigment pattern formation. *Development* 135:2603-14
145. Lynch JA, Peel AD, Drechsler A, Averof M, Roth S. 2010. EGF signaling and the origin of axial polarity among the insects. *Curr Biol* 20:1042-7
146. Futran AS, Link AJ, Seger R, Shvartsman SY. 2013. ERK as a model for systems biology of enzyme kinetics in cells. *Curr Biol* 23:R972-9
147. Stathopoulos A, Levine M. 2005. Localized repressors delineate the neurogenic ectoderm in the early Drosophila embryo. *Dev Biol* 280:482-93
148. Ajuria L, Nieva C, Winkler C, Kuo D, Samper N, et al. 2011. Capicua DNA-binding sites are general response elements for RTK signaling in Drosophila. *Development* 138:915-24
149. Cowden J, Levine M. 2003. Ventral dominance governs sequential patterns of gene expression across the dorsal-ventral axis of the neuroectoderm in the Drosophila embryo. *Dev Biol* 262:335-49
150. Kanodia JS, Kim Y, Tomer R, Khan Z, Chung KH, et al. 2011. A computational statistics approach for estimating the spatial range of morphogen gradients. *Development* 138:4867-74

FIGURE CAPTIONS

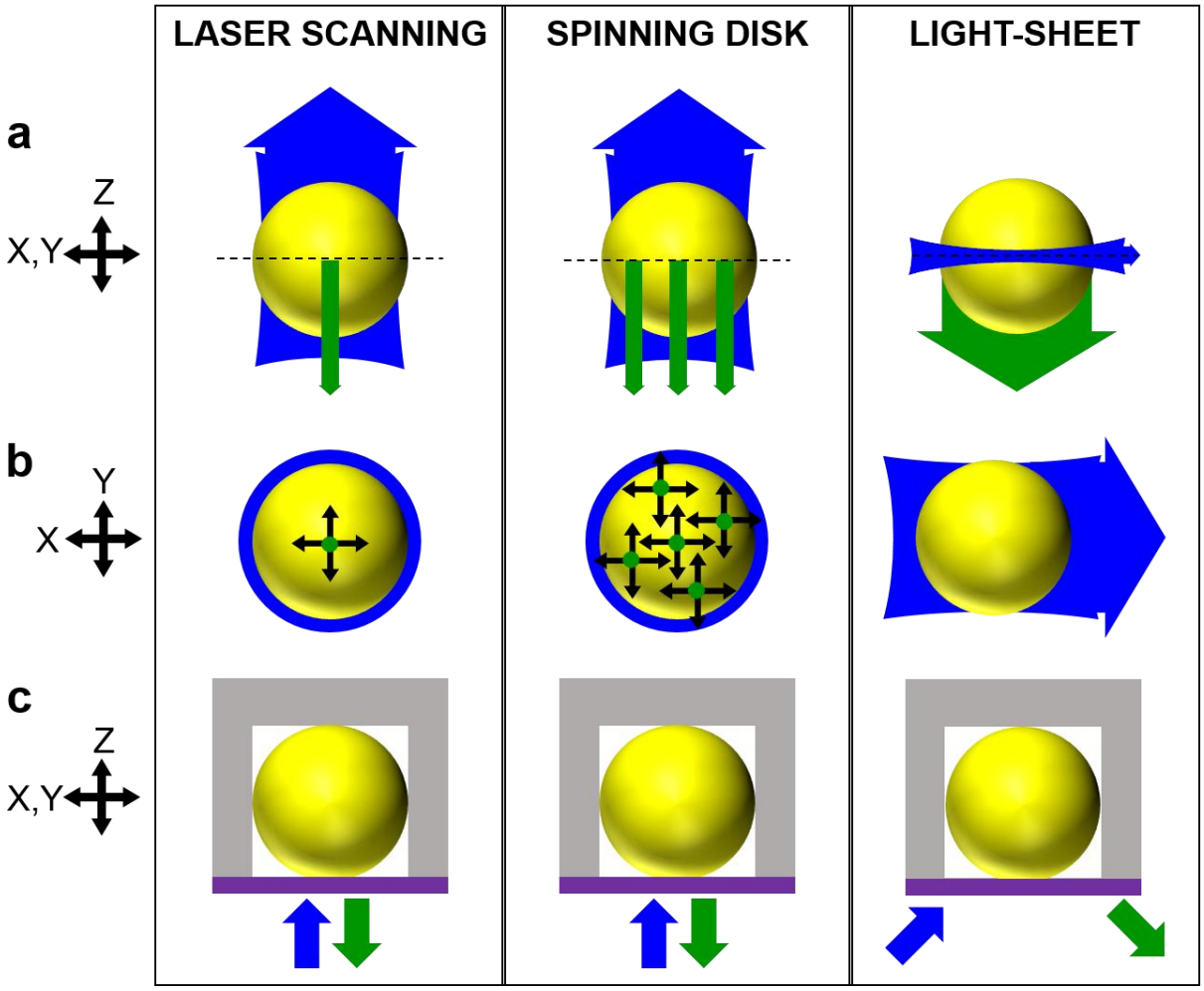

Figure 1

(a-c) Comparison of laser scanning confocal microscopy (left column), spinning disk confocal microscopy (middle column), and light-sheet microscopy (right column). (a) A schematic of the x,y-z plane cross section of a sample being imaged via 3 microscopy techniques. Blue represents illumination light, green represents emitted fluorescence, yellow represents biological sample, and black dotted line represents focal plane. Note: light-sheet microscopy illuminates only part of the specimen in the focal plane. (b) A schematic of the x-y plane cross section of a sample being imaged via 3 microscopy techniques. Laser-scanning requires the scanning of a single point to

construct an image. Spinning disk requires the scanning of multiple points to construct an image. Light-sheet microscopy with a real light-sheet does not require laser scanning. (c) A schematic of the x,y-z plane cross section of a biological sample being immobilized in a microfluidic device and imaged via 3 microscopy techniques. Gray represents top side of microfluidic device, usually polydimethylsiloxane, and purple represents the bottom imaging side of a microfluidic device, usually a glass cover slip. Light-sheet microscopy illuminates and detects at 45^{o} to the glass cover slip which causes unwanted optical aberrations.

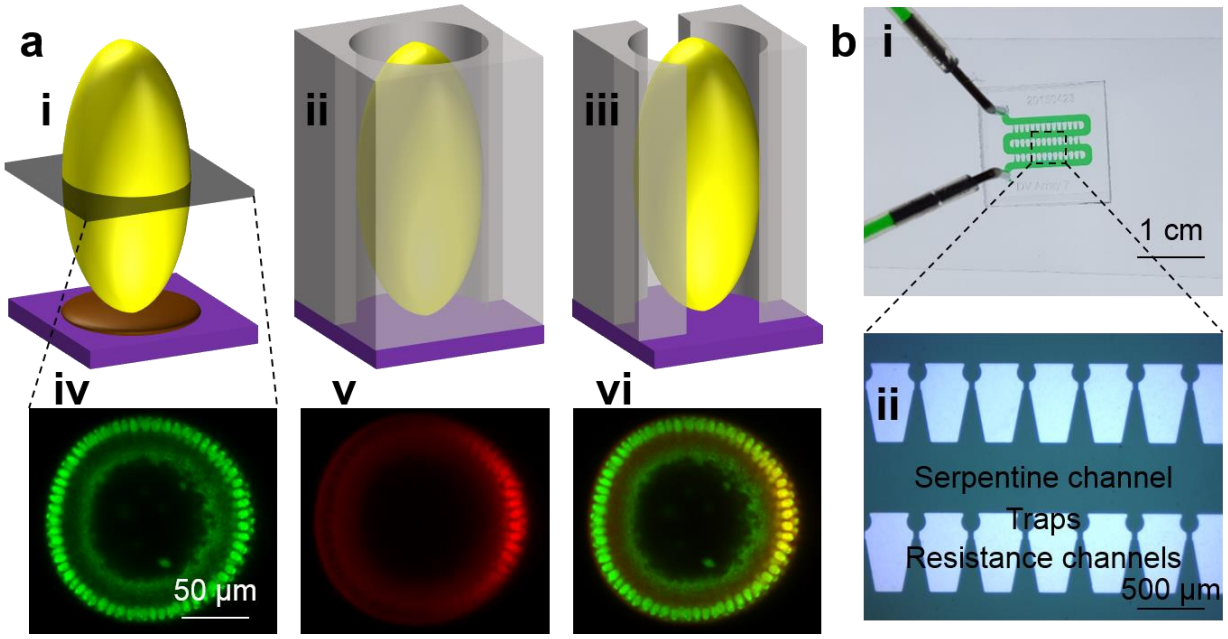

Figure 2

(a) End-on imaging of a *Drosophila* embryo via (i) manual orientation using glue (brown), (ii) manual placement into agar wells as described by Witzberger et al. , and (iii) using a microfluidic device for automated orienting and immobilizing *Drosophila* embryos for end-on imaging as described by Chung et al. (33). Yellow represents the *Drosophila* embryo, gray represents top side of microfluidic device, usually polydimethylsiloxane, and purple represents the bottom imaging

side of a microfluidic device, usually a glass cover slip. (iv-vi) Fluorescence images acquired via laser-scanning confocal microscopy of an end-on oriented embryo depicting (iv) histone-GFP, (v) Dorsal (Dl), and (vi) merged fluorescence. (b) (i) Optical micrograph of the microfluidic embryo trap array described in Levario et al. (40) with channels filled with green dye, and (ii) close-up of boxed-region in (i) depicting the features of the microfluidic embryo trap array.

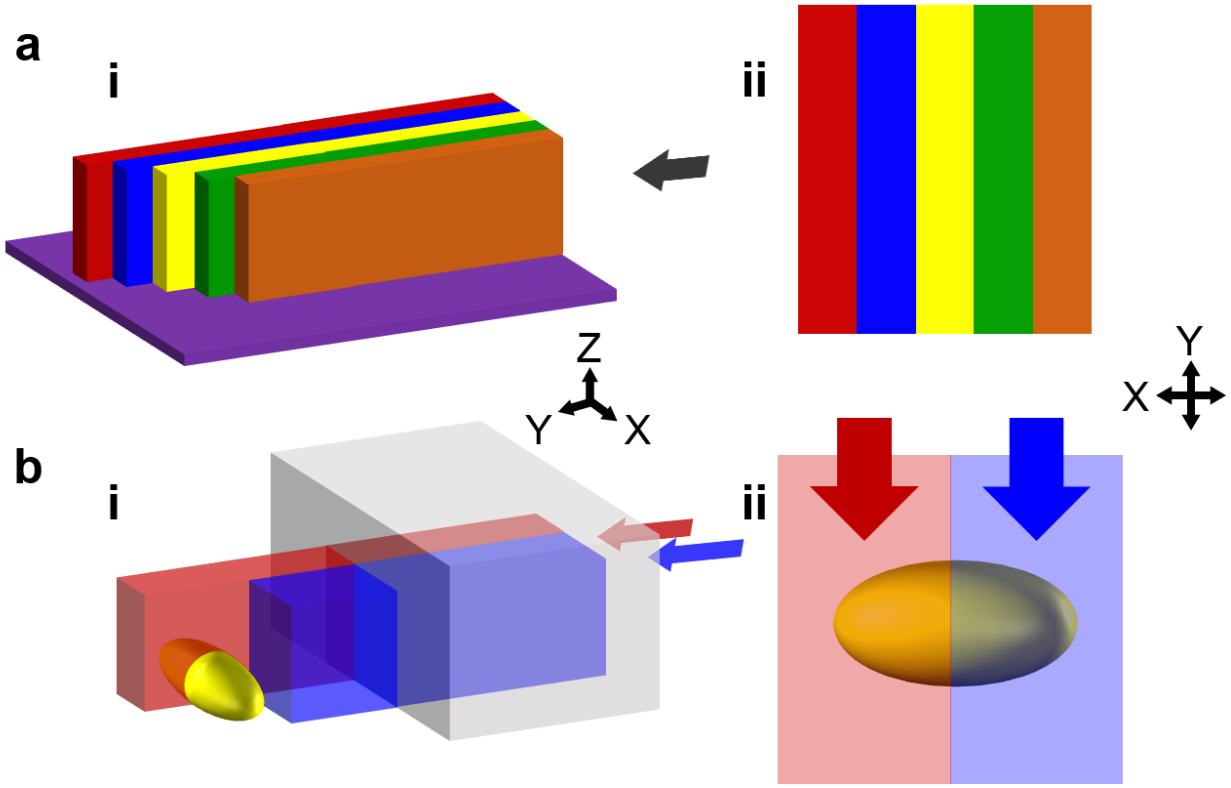

Figure 3

(a) A schematic diagramming laminar flow. (i) 3D representation. Gray represents top side of microfluidic device, usually polydimethylsiloxane, and purple represents the bottom imaging side of a microfluidic device, usually a glass cover slip. Adjacent "sheets" of fluid are depicted by individual colors (red, blue, yellow, green, and orange) indicating that during laminar flow fluid moves past each other like individual sheets. (ii) A cross section of the x-y plane. Convective

transport in the y-direction dominates the diffusive transport in the x-direction thereby allowing individual “sheets” or colors of fluid to flow past each other without mixing. (b) A 3D (i) and x-y cross section (ii) schematic of the experiment developed by Lucchetta et al. (36) that used a microfluidic device to expose a developing *Drosophila* embryo to a temperature-step. This was achieved by merging hot and cold fluids in a microfluidic channel, and the step-change is maintained via laminar flow and high Péclet number.

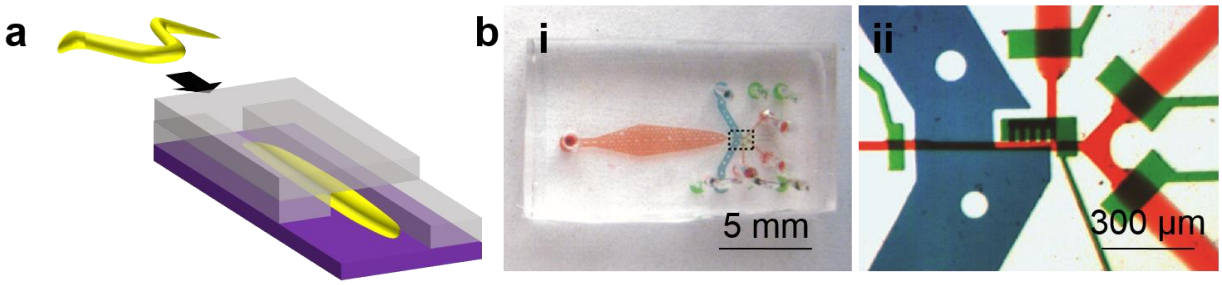

Figure 4

(a) A schematic of using physical confinement to immobilize physiologically active *C. elegans* without the need for anesthetics or glue. Yellow represents an individual *C. elegans*, gray represents top side of microfluidic device, usually polydimethylsiloxane, and purple represents the bottom imaging side of a microfluidic device, usually a glass cover slip. (b) (i) Optical micrographs of a dye-filled microfluidic device for sorting *C. elegans* as described by Chung et al. (81). (ii) Close-up of boxed region in (i). Red represents the flow channel where *C. elegans* are located, green represents control layer with on-chip valving to control fluid flow in the red channel, and blue represents the cooling channel that is used to cool *C. elegans* for immobilization during imaging.

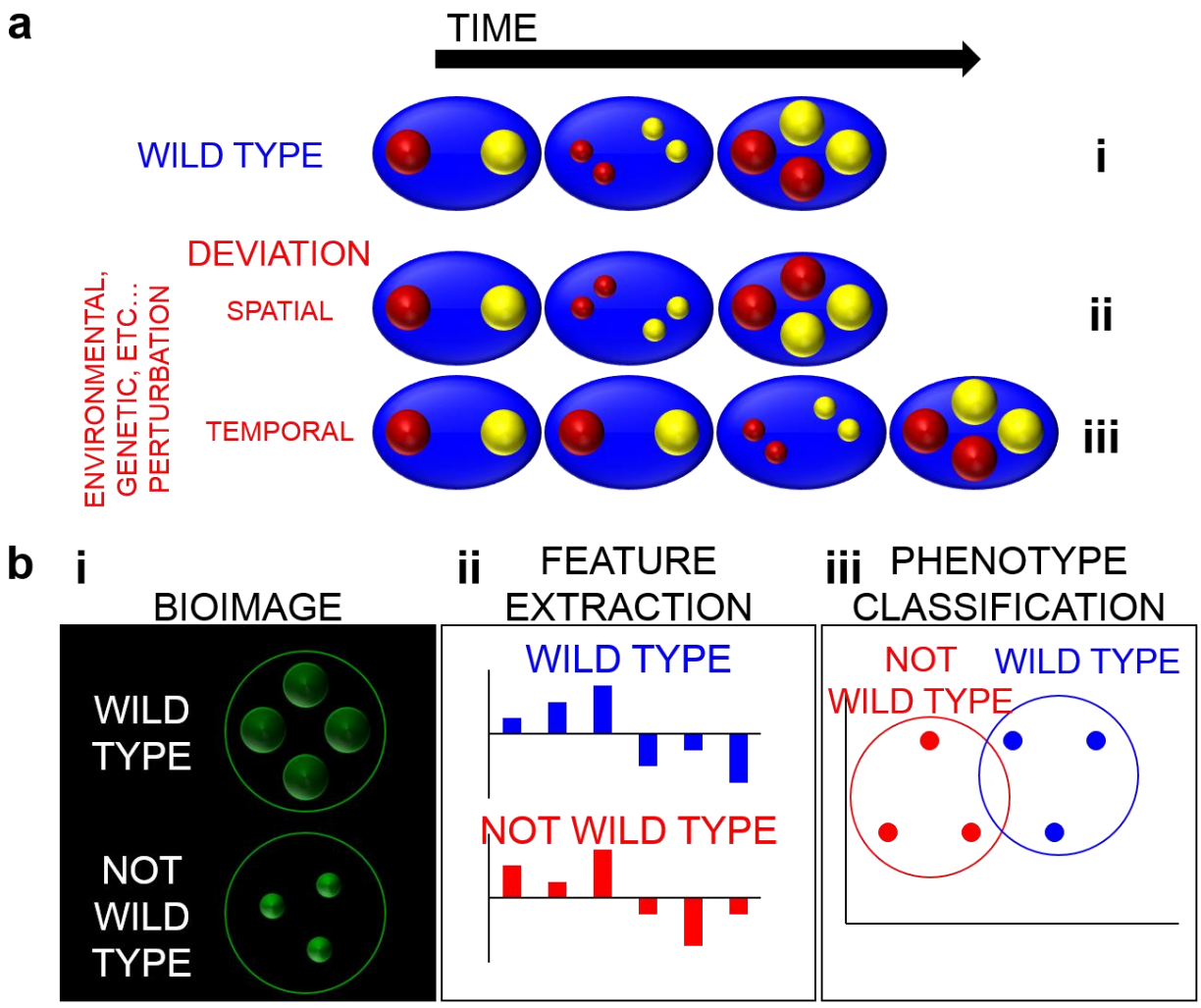

Figure 5

(a) Schematic diagramming concept of virtual embryo. (i) Depicts a wild type embryo starting at two cell-stage (red and yellow nuclei, blue cytoplasm), proceeding through a cellular division and ending at the four-cell stage. (ii) Depicts an embryo that phenotypical deviates from wild type as a result of a perturbation, and the deviation is spatial in characteristic as indicated by daughter cells incorrectly being spatially located in wrong areas within the embryo. (iii) Depicts an embryo that phenotypical deviates from wild type as a result of a perturbation, and the deviation is temporal in characteristic as indicated by the delayed nuclear division, yet daughter cells attaining the expected

spatial locations within the embryo. (b) Flow-chart diagramming the use of computer-vision for bioimage classification and automated phenotyping. (i) Diagram of two embryos depicting a wild type phenotype and one that deviates from wild type. (ii) Computer-vision can be used to extract features about the bioimage that can be used in (iii) a classification scheme that, in this case, can automatically distinguish wild type embryos from non-wild type based on features and cloud association. Note: The schematic depicts obviously different phenotypes, but computer-vision becomes powerful when subtle phenotypic changes are present.

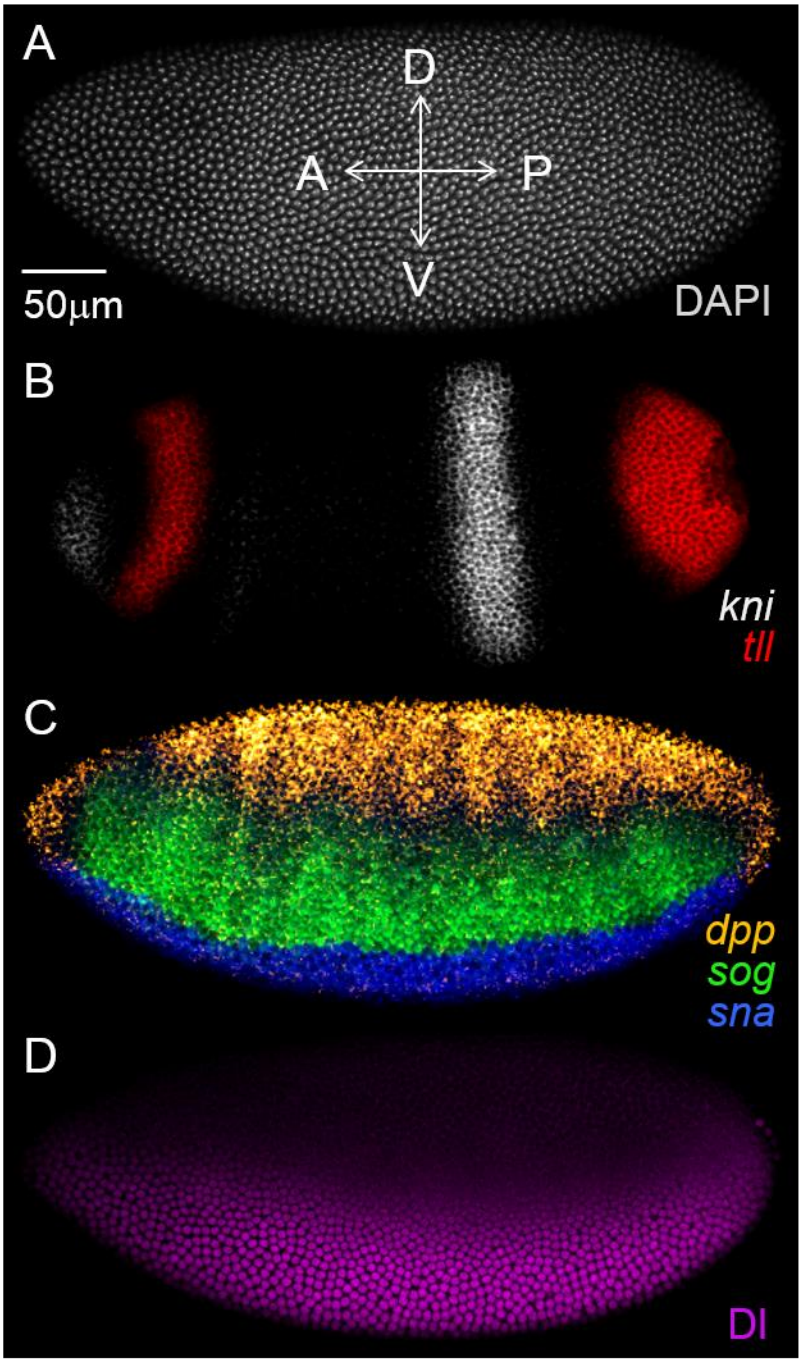

Figure 6

(a) A lateral surface view of early Drosophila embryo (~2.5hr after fertilization) stained with nuclei marker, DAPI. Nuclei are uniformly arranged in the periphery of an embryo. The embryo is positioned with its anterior side to the left and the dorsal side on top. (b) Embryo stained with AP

patterning genes, knirps (kni) and tailless (tll). (c) Embryo stained with DV patterning genes, decapentaplegic (dpp), short gastrulation (sog), and snail (sna). (d) Nuclear Dorsal gradient controls the DV patterning of the embryo.

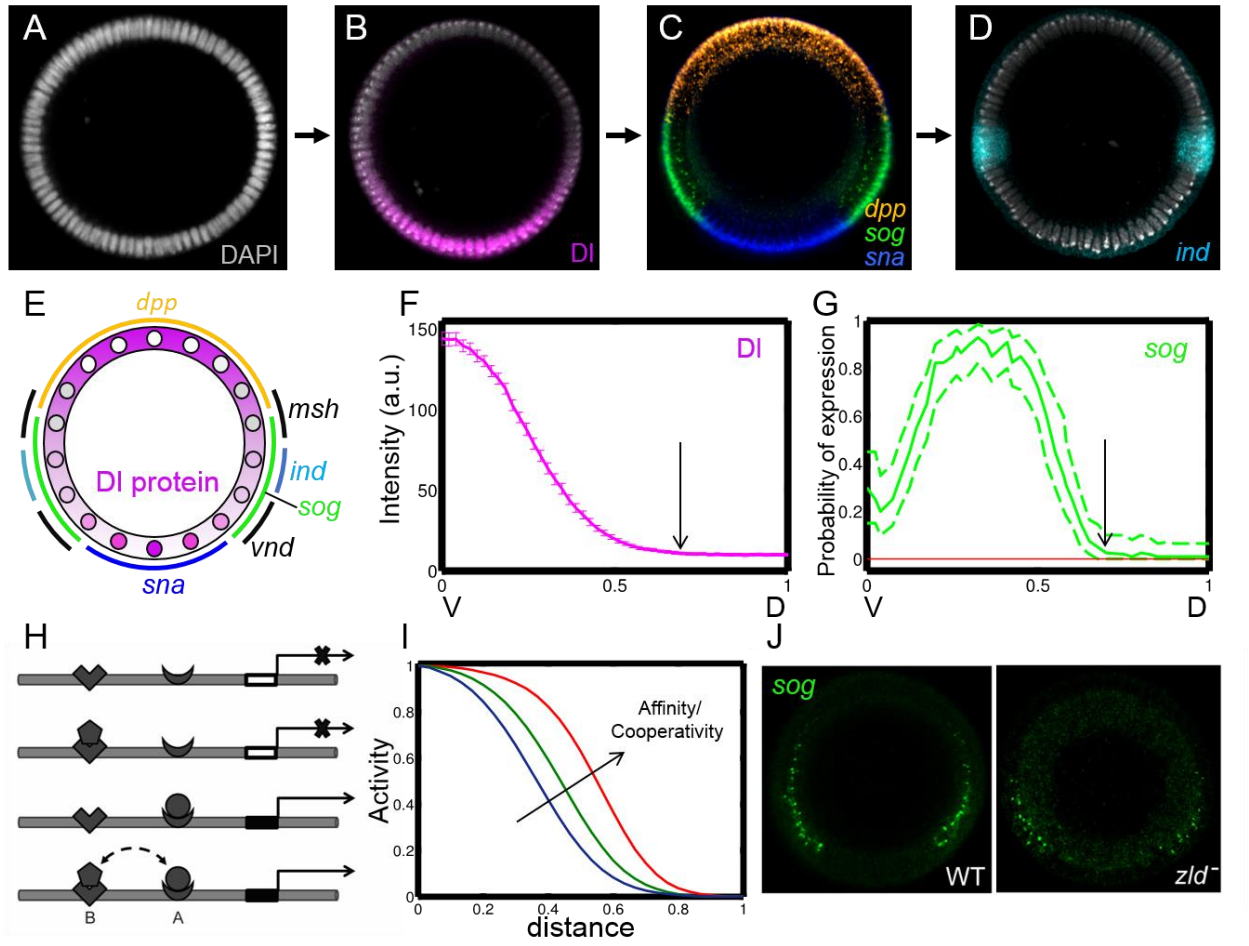

Figure 7

(a-d) Optical cross-sections of early *Drosophila* embryos can be obtained by using the microfluidic embryo trap-array (33). From a uniform sheet of nuclei (grey) (a), a graded signal (Dorsal – magenta) (b) is induced to subdivide the embryo into three parts, each of which will become future muscle (snail – blue), nerves (sog – green), and skins (dpp – orange), in concentration dependent manner (c). Each of this section can be specified even further by a secondary signaling. For

example, ind (cyan) (d) is expressed within the future nervous system region, to induce specific cellular fate of intermediate neuronal stem cells. (e) Nuclear Dl gradient directly or indirectly establishes the gene expression borders along the dorsoventral (DV) axis of embryos. (f) Average nuclear Dl gradient along the DV axis (n=23). The arrow represents the estimated range of nuclear Dl gradient. The errorbar represents to the standard error of the mean. (g) Mean sog expression profile along the DV axis (n=68). Dashed lines indicate the 99% Bayesian confidence interval. The arrow indicates the estimated range of sog expression (0.66). (h) Schematic of the gene regulation model by the graded (a) and the uniform (b) signal. (i) Gene expression domains change with respect to changes in the binding affinity and the cooperativity between the two factors shown in (e). (j) Expression of sog nascent transcripts in wild type and in zelda-/- embryos along the DV axis. The sog expression level is lower, and the expression boundary is narrower in zld-/- embryos. Figure 1g is modified from (150), and 1H-J are modified from (126).

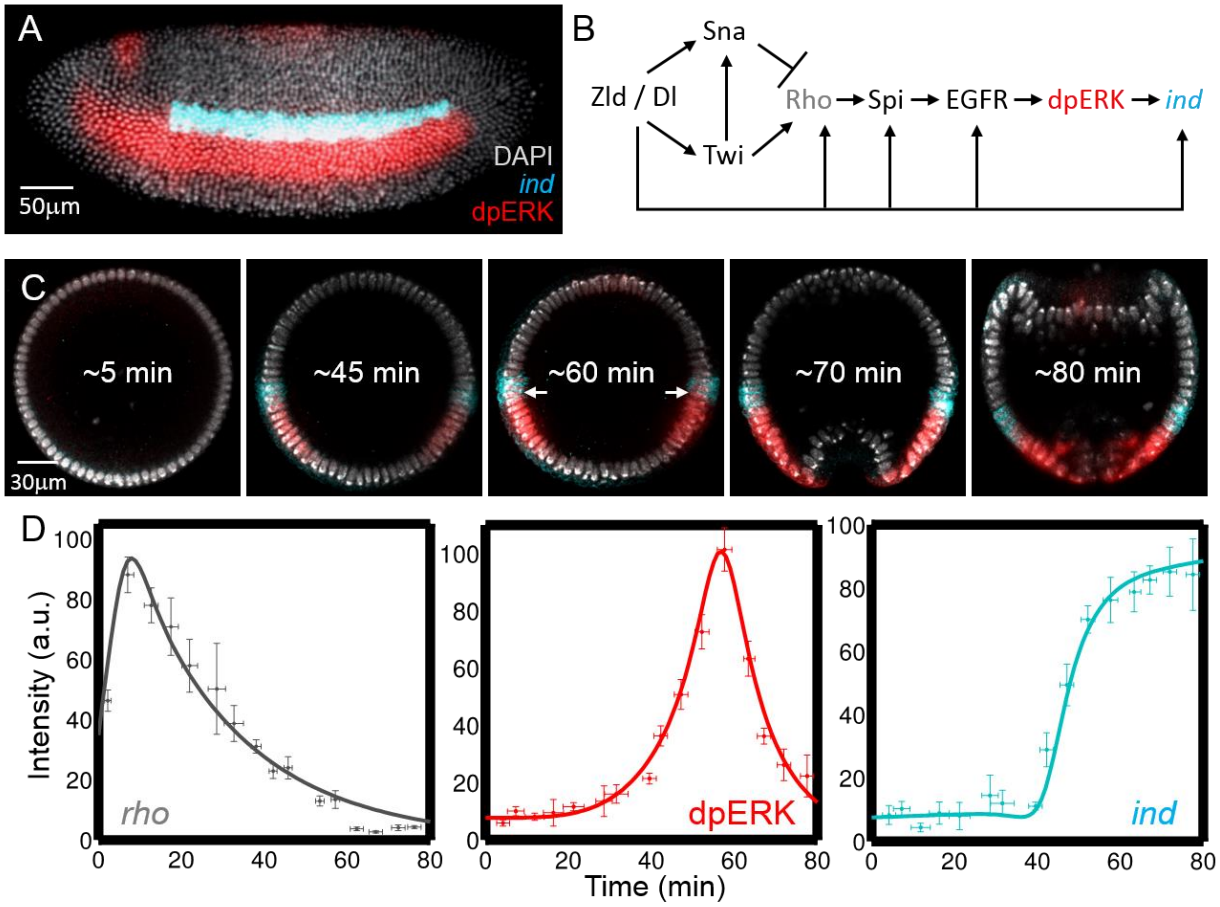

Figure 8

(a) A lateral view of early *Drosophila* embryo stained for nuclei (DAPI – grey), dpERK (red), and ind mRNA (cyan). (b) Gene regulatory network that leads to the induction of ind. (c) Optical cross-sections of embryos stained for DAPI, dpERK, and ind mRNA are ordered in time (0min corresponds to the onset of nuclear cycle 14, ~2hr after fertilization). The arrows indicate the position where the signal was extracted for quantification in (d). (d) Dynamics of rho, dpERK, and ind expression in the cell where ind is being expressed (arrows in (c)). rho is expressed first, and the expression level decreases over time. ERK is activated as a pulse ~40min after the onset of cycle 14, and then ind is induced in a switch-like manner, shortly after ERK activation. Figure 2a, c, d are modified from (130).